1992

Interfacial electrochemical studies of adsorbates on polycrystalline and single crystal electrodes

Gary Lawrence Borges
San Jose State University

Order Number 1350069

Interfacial electrochemical studies of adsorbates on polycrystalline and single crystal electrodes

Borges, Gary Lawrence, M.S.

San Jose State University, 1992

U·M·I

300 N. Zeeb Rd.
Ann Arbor, MI 48106

INTERFACIAL ELECTROCHEMICAL STUDIES OF ADSORBATES ON POLYCRYSTALLINE AND SINGLE CRYSTAL ELECTRODES

A THESIS
PRESENTED TO
THE FACULTY OF THE DEPARTMENT OF CHEMISTRY
SAN JOSE STATE UNIVERSITY

IN PARTIAL FULFILLMENT
OF THE REQUIREMENTS FOR THE DEGREE
MASTER OF SCIENCE

BY
GARY LAWRENCE BORGES
AUGUST, 1992

APPROVED FOR THE DEPARTMENT OF CHEMISTRY

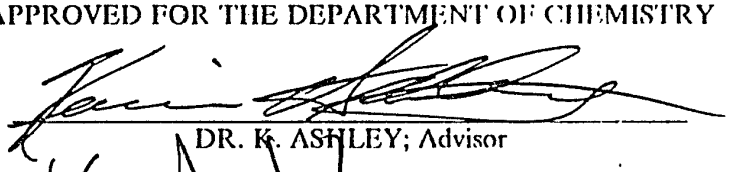

DR. K. ASHLEY; Advisor

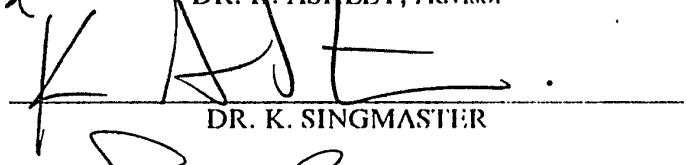

DR. K. SINGMASTER

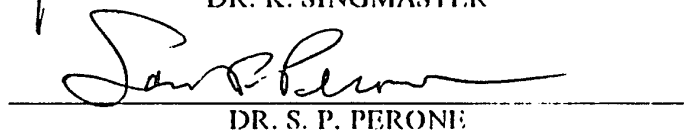

DR. S. P. PERONE

APPROVED FOR THE UNIVERSITY

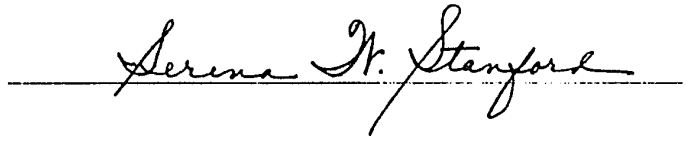

ABSTRACT

INTERFACIAL ELECTROCHEMICAL STUDIES OF ADSORBATES ON POLYCRYSTALLINE AND SINGLE CRYSTAL ELECTRODES

BY GARY LAWRENCE BORGES

Interfacial electrochemistry is the topic of a three part investigation into the fundamental events occurring at the metal electrode/electrolyte interface.

Optical second harmonic generation(SHG) and quartz crystal microbalance(QCM) techniques are used as in-situ probes of copper underpotential deposition (UPD) on polycrystalline gold surfaces in sulfuric acid. The SHG signal from a polished gold electrode is observed to decrease by >60% as a result of copper UPD. Also, the mass of a UPD adlayer is monitored by an oscillating QCM, yielding an estimated coverage of ca. 8.0 x 10^{-10} mol/cm^2 and an electrosorption valency of 1.5 for a copper adlayer on the polycrystalline gold.

The preparation of evaporated thin films of largely single crystalline copper is reported. Most of the Cu surface has (111) orientation, as established by X-ray scattering and electrochemical studies. The (111) surface domains are on the order of 300 Å in diameter and have a mosaic spread of ca. 0.1 °. UPD shifts for Pb and Tl on these Cu(111) films are approximately 150 and 300 mV, respectively.

The evaporation of Au thin films onto the QCM at high temperatures results in largely crystalline Au(111) electrodes as determined electrochemically by Cu UPD in sulfuric acid. In-situ electrochemical/QCM studies for sulfuric acid(no copper) detect the adsorption/desorption of a monolayer's worth of surface bound sulfate(18 Hz) from the Au(111) surface. For Cu UPD in sulfuric acid, sulfate desorption appears, followed by the adsorption of a monolayer of Cu(33 Hz) and a co-adsorbed monolayer of sulfate(18 Hz).

Acknowledgments

The author would like to thank Dr. Kevin Ashley for his guidance, expertise, and support throughout this endeavor. The author also acknowledges, and thanks the following collegues for their support:
Dr. Bradley Stone, Mark Lazaga (Dept. of Chemistry), Dr. Sarma Lakkaraju, Mark J. Bennahmias, (Dept. of Physics); San Jose State University, San Jose, CA 95192

Dr. J. G. Gordon II, Dr. Mahesh G. Samant, Dr. Kay K. Kanazawa Dr. Erwin Holland-Moritz(STM); Ofelia Chapa-Perez(technical assistance). IBM Research Division, Almaden Research Center, San Jose, CA 95120.

The Author wishes to thank the Optical Society of America for permission to reproduce Chapter II of this thesis.

Table of Contents

Chapter I. INTRODUCTION TO SURFACE ELECTROCHEMISTRY

The innovations of in-situ techniques specific for the characterization of surface properties are stimulating a great deal of interest in and research on the electrochemical interface. The goal of this research is to understand the fundamental events occurring at the electrode surface, and to study in more detail the reactions occurring at the interface. Interfacial phenomena play a major role in the application of a variety of technologically important materials, where surface phenomena such as corrosion, adhesion, and catalysis are important. For the electrochemical interface, the process of underpotential deposition(UPD) of a monolayer, or a submonolayer of an adsorbate on a metallic electrode has been intensively studied, owing to the theoretical interest and the practical consequences for many fields such as surface chemistry, electrocrystallization, electrocatalysis, and electroplating. It is essential to use in-situ techniques to study such adsorbates at the electrochemical interface in an effort to determine directly their structure, oxidation state, and the interfacial enviroment in which they exist.

Standard electrochemical techniques provided the initial studies from which a model describing the electrochemical interface was first envisioned. A popular model of the interface which survives today is called the Gouy-Chapman-Stern(GCS) model of the electrochemical interface(1). This model supports the evidence that the electrode, the crystallinity of exposed crystal face and adsorption all have profound influence on the chemical and physical properties of the interface. This classical model for the interface includes the influence of ions and molecules, both adsorbed and nonadsorbed at the electrode surface, and the processes observed there e.g., electron transfer, ionic effects,

H-bonding, etc. The GCS model goes further to depict, in atomic detail, the role that the ions and solvent molecules play. The model includes interactions of solvents, ions, adsorbates, etc. at and near the electrode surface under the influence of an applied potential. The model yields a Galvani potential profile beginning at the electrode surface, on out into the diffuse layer (where non adsorbed ions are under the influence of the electrode's potential), and into the bulk electrolyte. This picture of the electrochemical interface is drawn largely from the prodigious collection of traditional electrochemical measurements of current, voltage, charge, and capacitance. In truth, the GCS model can only account for the gross features of behavior in real systems at the electrochemical interface. The detailed atomic events occurring at this interface is largely beyond the scope of the GCS model, i.e., the GCS model is a macroscopic model of the electrochemical interface.

With the advances in surface sensitive probes and techniques (e.g. low energy electron diffraction(LEED), Auger, X-rays, etc.), especially those surface techniques capable of atomic resolution, and the huge impact they have had on studies of the solid/gas(vacuum) interface, electrochemists and others began to look for ways to apply these techniques to the electrochemical interface. These surface sensitive techniques could potentially resolve the atomic structure of the electrochemical interface providing valuable, fundamental details of electrode/solution interfaces. Furthermore, these methods can be used to verify and perhaps improve upon the GCS model of the interface.

The first attempts to bring surface sensitive probes capable of structural determination to interfacial electrochemistry were ex-situ experiments in which the electrode was removed from the electrochemical cell and put into a vacuum to be examined with electron or ion beams(2). These ex-situ experiments did

provide structural detail of the interface, but the loss of potentiostatic control and exposure to the vacuum enviroment raised questions as to the integrity of the electrochemical interface. The inherent assumption of these ex-situ techniques is that the electrochemical interface is still intact even after the electrode is removed from solution. In many cases, especially at potentials far from the potential of zero charge(pzc), this assumption may not be reasonable. Clearly, an in-situ structural determination is preferred in order that structural rearrangements of the interface do not occur in transfering the electrode from cell to vacuum.

For in-situ surface sensitive probes of the electrochemical interface, researchers have used optical techniques (UV-Vis Spectroelectrochemistry(3), Fourier Transform IR Spectroscopy(4), Surface Enhanced Raman Scattering(5), Second Harmonic Generation(SHG)(6), Attenuated Total Reflection Spectroscopy(ATR)(7)), high energy probes like X-ray fluorescence(8) and diffraction(9), and a few other exotic techniques such as scanning tunneling microscopy(STM)(10), radioisotopic labeling(11), and quartz crystal microbalance(QCM)(12). Surface sensitive optical techniques by and large measure interfacial presence, reaction mechanisms, and the kinetics involved there. X-ray techniques, by the virtue of their short wavelengths, have shown the atomic arrangement of the electrochemical interface. The remaining surface sensitive techniques which have been employed have their own unique contribution to interfacial studies. For example, using isotopically labeled ions, Wieckowski et al. detects and measures the coverage of species adsorbed to different electrodes as a function of the applied potential(11). The QCM has been shown to be sensitive enough to weigh in-situ a mono-atomic layer(monolayer) of adsorbed metal ions that were reduced onto an electrode(12). For the electrochemical STM, the remarkable atomic images of Cu adatoms on a Au(111)

electrode by Behm et al. can be considered a major contribution to electrochemical interfacial research(13).

Currently, electrochemical interfacial studies are enjoying a renaissance in regards to experimental methodology employing surface sensitive techniques. Combined with the progress in new approaches to control the atomic architecture at the interface, these surface sensitive techniques hold much promise for revealing the atomic events taking place at the electrochemical interface. The goal of this research is to develop and apply a few state of the art techniques which could provide insights to future interfacial studies, and to build a level of confidence for applying other, more powerful surface sensitive probes to those systems that are thought to be interesting. These in-situ surface sensitive probes would be powerful enough to provide chemical characterization and structural information for a complete description of the interface, to the atomic level.

UPD Monolayers and Single Crystal Electrodes

The initial deposition of an atom(adatom) onto an electrode followed by the nucleation and growth of the adatom phase on the surface of the electrode is a fundamental interfacial event still being studied by electrochemists. With the discovery of systems where a monolayer worth of adsorbed metal atoms(adatoms) can be deposited onto a foreign metal electrode at potentials positive of the Nernstian potential(14,15), it was possible for electrochemists to study these intial interfacial events. The deposition of a stable monolayer, known as underpotential depositon(UPD), has been studied extensively by electrochemical, optical and other surface sensitive techniques.

To further simplify the picture and gain insights to the local atomic environment and the events taking place during adsorption and interfacial

deposition e.g. UPD, it would be ideal to use an electrode whose surface is uniformly homogeneous to the adatom phase. An electrode surface which is uniformly homogeneous to a monoatomic adatom phase suggests a surface which is atomically smooth and ordered, or crystalline. Such a requirement is filled by the use of carefully cut, polished, and cleaned single crystal metal electrodes. Single crystal electrodes are much more difficult to fabricate and handle compared to the polycrystalline form. However, it is known from studies using single crystal electrodes, that the UPD of adatoms is very sensitive to the crystal orientation of the electrode surface(14). This demonstrates the utility of an electrode surface which is atomically smooth, and whose surface structure is well characterized.

This Work

Interfacial electrochemistry is the topic of a three part investigation into the fundamental events occurring at the interface between the metal electrode and the electrolyte. The body of research presented here describes experiments that probe for insights into these fundamental interfacial events. All three chapters employ voltammetry, which allows modification of the electrochemical interface by applying a potential(voltage) to a metal electrode immersed in a chemical system of interest. In other cases, voltammetry (cyclic voltammetry) is used to characterize the electrode surface which was prepared, i.e. crystalline or polycrystalline.

The first of these studies is an effort employing the preparation of thin film polycrystalline electrodes to study interfacial events with the Quartz Crystal Microbalance(QCM) and by Second Harmonic Generation(SHG), a surface sensitive optical probe(6). SHG is a surface sensitive probe which is not fully

understood, especially when applied to the electrochemical interface. An intuitive description of the surface term of the source polarization for the SHG signal that is responding to changes at the electrochemical interface is not available. It is known that only the surface term for the SHG intensity comes from structural and field discontinuities at the electrode surface. In combining the QCM with SHG experiments, the interfacial events for monolayer adsorption/desorption which were detected by the QCM greatly altered the SHG signal coming from this interface.

The second study describes a method for the preparation of thin film Cu(111) electrodes and their structural and electrochemical characterization. Cu(111) is another single crystal electrode surface which will be used in future X-ray experiments to measure the structure of the electrochemical interface. We are interested in investigating the structural interfacial changes for these Cu(111) electrodes with respect to adsorption of metals, electrolytes and other ions, molecular species, and electrode roughening and oxide growth. By detailing our procedure for evaporating thin film Cu(111) and having characterized the Cu(111) surface both structurally and electrochemically, we hope other researchers will find other important applications for these films either in research or in technological applications.

The third and final study extends our application of thin film electrodes to the preparation of thin film single crystal gold electrodes(determined electrochemically) on the QCM. This is a unique demonstration of a highly crystalline (111) electrode on the QCM. The results obtained from the QCM, where UPD of Cu in sulfuric acid on the thin film Au(111) electrode is investigated, are quite complex. A model for the UPD of Cu on Au(111) in sulfuric acid is proposed which is consistent with the data. The complex nature

of the events leading to the formation of a Cu monolayer on the Au(111) electrode is also described in the literature. Initial STM results show at least two atomic phases of Cu growing on the Au(111) surface(13). In a recent paper these different Cu phases were not seen; only a simple $\sqrt{3}$ x $\sqrt{3}$ Cu adlayer commensurate with the Au(111) lattice was found by the STM(16). Conflicting SEXAFS results show the UPD monolayer to be either Cu(0)(8) on the Au(111) surface or Cu(I)(17), with SO_4^{-2} and HSO_4^- present at the interface to varying extents. From IR measurements of the interface, the Cu UPD adlayer is surrounded by sulfate, and possibly bisulfate anions, with surface bound water molecules nearby(18). Much interesting interfacial research on this system has produced inconsistent results. Hence, one can expect to see a great deal more research in the near future as researchers attempt to resolve the inconsistencies found in the current literature for Cu UPD on crystalline gold electrodes.

This thesis is a collection of studies where the author's contribution lies largely in the electrochemistry and the quartz crystal microbalance(QCM) techniques which were needed to characterize the interface. The preparation of thin film polycrystalline and single crystal electrodes is also presented. Using thin film evaporation techniques, we were able to produce crystalline and polycrystalline metal electrodes (Au, Ag, Cu, Pt) of useful sizes and shapes as required by the experiment, and in large numbers. From the inherent cleanliness of the UHV evaporation process, these electrodes were pristine in nature and used without further handling or modification in each of these studies. These electrodes were then used to study fundamental interfacial processes while under electrochemical control.

References

1. A. J. Bard and L. R. Faulkner, **Electrochemical Methods: Fundamentals and Applications** J. Wiley & Sons, New York, 1980, Chapter 12 and references therein.

2. A. T. Hubbard, **Acc. Chem. Res.** 13, 177 (1980).

3. W. R. Heineman, F. M. Hawkridge, and H. N. Blount, in **Electroanalytical Chemistry**, Vol. 13; A. J. Bard(ed.). Dekker, New York, 1974, and references therein.

4. K. Ashley and S. Pons, **Chem Rev.** 88, (1988) 673-695.

5. R. K. Chang and T. E. Furtak(eds.), **Surface Enhanced Raman Scattering**, Plenum Press, New York, 1982.

6. G. L. Richmond, J. M. Robinson, and V. L. Shannon, **Prog. Surf. Sci.** 28, (1988) 1-70.

7. D. B. Parry, J. M. Harris, and K. Ashley, **Langmuir** 6, (1990) 209-217.

8. L. Blum, H. D. Abruna, J. White, J. G. Gordon, G. L. Borges, M. Samant,and O. R. Melroy, **J. Chem. Phys.** 85, no. 11 (1986) 6732-7.

9. M. G. Samant, M. F. Toney, G. L. Borges, L. Blum, O. R. Melroy, **J. Phys. Chem.** 92, (1988) 220-5.

10. R. Sonnenfeld, J. Schneir, P. K. Hansma, in **Modern Aspects of Electrochemistry**, R. E. White, J. Bockris, B. E. Conway(eds.), Plenum Press, New York, 1990; Vol. 21.

11. P. Zelenay, L. M. Rice-Jackson, A. Weickowski, **Surface Science** 256, (1991) 253-263.

12. O. R. Melroy, K. K. Kanazawa, J. G. Gordon, and D. Buttry, **Langmuir** 2, (1986) 697-700.

13. O. M. Magnussen, J. Hotlos, G. Beitel, D. M. Kolb, R. J. Behm, **Phys. Rev. Lett.** 64, (1990) 2929.

14. D. M. Kolb, **Advances in Electrochemistry and Electrochemical Engineering**, , Vol. 11, Ch. 2, P. Delahay(ed.), J. Wiley & Sons, New York, 1977.

15. W. J. Lorenz, I. Moumtzis, and E. Schmidt, **J. Electroanal. Chem.** 33, (1971) 121-133.

16. T. Hachiya, H. Honbo, and K. Itaya, **J. Electroanal. Chem.** 315, (1991) 275-291.

17. A. Tadjeddine, G. Tourillon, and D. Guay, **Electrochim. Acta.** 36, No. 11/12, (1991) 1859-1862.

18. D. Parry, M. G. Samant, H. Seki, M. R. Philpott, K. Ashley, in preparation.

Chapter II. COMBINED OPTICAL SECOND HARMONIC GENERATION/QUARTZ CRYSTAL MICROBALANCE STUDY OF UNDERPOTENTIAL DEPOSITION PROCESSES: COPPER ELECTRODEPOSITION ON POLYCRYSTALLINE GOLD

Introduction

In the past decade a number of surface-sensitive in situ(i.e. in solution) optical techniques, such as infrared(IR) spectroelectrochemistry(1,2) and optical second harmonic generation(3,4), have been used to probe the interface between an electrode and an electrolyte solution. Second harmonic generation and more generally sum frequency generation(SFG) techniques, being surface specific and monolayer sensitive, can be used to interrogate the structure of the interface between a metal and liquid in electrochemical and other systems(5). Further spectroscopic methods that have been applied to the in situ study of electrochemical interfaces include in situ x-ray techniques(6), such as surface extended x-ray absorption fine structure(SEXAFS) and surface-enhanced Raman scattering(SERS)(7). In addition to advances in the spectroscopy of surfaces in electrochemical systems, the oscillating quartz crystal microbalance(QCM), which is extremely sensitive to the mass adsorbed species on an electrode surface, has been used successfully in a number of electrochemical applications(8). The QCM has been used in situ to investigate a variety of interfacial processes such as ion flux through polymers(9,10), film formation(11), and ionic adsorption(12), among other phenomena. The mass sensitivity of the QCM utilized in solution is reportedly the same as that obtained in vacuum(13).

It is typically beneficial to examine interfacial electrochemical processes in situ since the environment of the electrode surface may undergo drastic changes if the

electrode is removed from solution and subsequently studied by conventional ex situ(either in air or in vacuum) methods. For example, in investigations of metal underpotential deposition(UPD) processes(where the metal adlayers become adsorbed to the electrode surface at electrode potentials which are insufficient to cause bulk metal deposition), substantial surface restructuring may occur if the electrode is removed from solution. Therefore, the development of in situ interfacial probes of electrochemical systems has recieved a great deal of attention in recent years. To this end, in this chapter in situ optical spectroscopic and mass-sensitive techniques were utilized which are responsive to the presence of underpotentially deposited adlayers on an electrode surface.

Second harmonic generation(SHG) is one of the second-order nonlinear optical phenomena that is forbidden (in the electric dipole approximation) in bulk materials having inversion symmetry. Since inversion symmetry is necessarily broken at an interface separating two distinct media, such as in an electrode-electrolyte system in electrochemistry, it is possible for a second harmonic signal to be generated from such interfaces(14). As a consequence SHG is intrinsically surface sensitive, as opposed to other optical methods like Raman scattering and infrared spectroscopy. The intensity of the second harmonic(SH) signal generated is proportional to the square of the second-order source polarization at twice the frequency(2ω) induced by the incident field at the fundamental frequency(ω). This source polarization can be conveniently written as(15,16):

$$P(2\omega) = P_s(2\omega) + P_b(2\omega),$$

where $P_s(2\omega)$ is the polarization produced by the surface (or interfacial region) and $P_b(2\omega)$ is due to the bulk material. The surface term, which invariably has some bulk contribution, comes from structural and field discontinuities at the

surface. The bulk contributions may be due to bulk having no inversion symmetry, although the contribution from this is zero in the experimental results reported here. In the particular case of electrochemical systems, the bulk term may have a contribution from the third-order nonlinearity due to the strong dc field within the double layer. The contribution from the surface term can, in general, involve a dipole allowed contribution as well as a quadrupole component due to field variation near the surface. The local and nonlocal contributions to the surface term are, generally speaking, of the same order of magnitude unless strongly nonlinear molecules are adsorbed on the surface. In our experiments there are no strongly nonlinear molecular adsorbates. Hence, the changes in second harmonic generation from our system are due principally to changes in the nonlinearity of the bulk material evidenced by the nonlocal response. Generally speaking, the bulk and surface contributions cannot be separated(17).

The quartz crystal microbalance(QCM) has been shown to be useful for the quantitative determination of submonolayer quantities of adsorbed species, even in an <u>in situ</u> environment, such as an electrochemical cell(8). In general, the mass change at an interface is related to the change in QCM oscillator frequency through the Sauerbrey equation(18):

$$\Delta f = -2\,\Delta m\, n\, f_o^{\,2} / (A(\mu_q \rho_q)^{1/2}) .$$

Here, Δf is the change in oscillator frequency, Δm is the change in interfacial mass, n is the overtone number(equal to unity for this work), f_o is the QCM fundamental frequency(5 Mhz for this work), A is the unit area of the oscillator, μ_q is the shear modulus of quartz(2.947x1011 g/cm s^2), and ρ_q is the density of quartz(2.648 g/cm^3). Use of a special QCM design enables applicability of the Sauerbrey equation to adlayers of uniform thickness(12) and yields an approxi-

mate QCM mass sensitivity of 18 ng/cm^2 for a crystal operated at 5 MHz. Even greater sensitivities are attainable for quartz crystals operated at higher frequencies.

In situ SHG and QCM techniques have been used recently in studies of UPD processes on but a few types of electrode surface. For example, SHG studies have been conducted on thallium UPD on gold and silver(19,20) and QCM techniques have been used to probe UPD of several metals on gold surfaces in perchloric acid(21). This work represents an effort to combine these two surface-sensitive methodologies to investigate copper UPD on polycrystalline gold substrates in sulfuric acid medium.

Experimental

Electrochemistry

For the SHG experiments, a gold mirror working electrode was prepared by mechanical polishing with successively smaller grades of polishing alumina(Buehler) of first 1.0-μm, then 0.3-μm, and finally 0.05-μm diameter. The gold electrode was then rinsed thoroughly with triply distilled, deionized water, and inserted into a spectroelectrochemical cell which was modified from a cell designed previously for reflectance IR spectroelectrochemistry(22). The mirror electrode was positioned 1-2 mm from the fused quartz cell window, which was held onto the face of the cell body(Kel-F) by an O-ring seal. A Ag/AgCl micro-reference electrode(Microelectrodes, Inc.) was positioned $\simeq$1 mm from the edge of the working(mirror) electrode. A platinum secondary (counter) electrode was placed behind the gold mirror electrode, as described in previous work(1,2,23). Copper sulfate (99.999%, Aldrich Gold Label) and sulfuric acid(G. F. Smith, doubly distilled) were used as recieved. All the solutions were degassed with nitrogen(99.999%) or argon(99.999%) before each experiment.

For cyclic voltammetry, the electrode potential was controlled with a waveform programmer/potentiostat system (either JAS instruments or Princeton Applied Research 175/179), and voltammograms were recorded on an X-Y plotter(IBM 7424MT or Houston Instruments 2000). In these experiments, the gold working electrode was pulled back from the quartz window(ca. 50 mm) to increase the distance between the gold surface and the window. The gold electrode surface was further polished electrochemically by repeated potential cycling prior to recording of SH signal intensity.

Second Harmonic Generation

The experimental apparatus for these SHG studies has been described previously(24). A Q-switched Quantel Nd:YAG laser was used to generate the second harmonic signal at the electrode surface using p-polarized 1.064 μm radiation. The pulse width was 12 ns and the repetition rate was 5 Hz. The fundamental beam was directed onto the surface of the gold mirror(working) electrode at a 45° angle of incidence following passage through two crossed polarizers for intensity reduction. A telescope was employed to reduce the beam size: the beam diameter was 3 mm at the electrode surface, and the energy per pulse was ca. 8 mJ. Radiation at the second harmonic frequency in the incident beam(mainly arising from the flashlamps of the laser) was eliminated by a filter. There were no thermally induced changes detected nor damage observed from exposure to laser pulses at the gold electrode surface.

The SH signal was collected (with no polarization selection) perpendicular to the fundamental beam (near the direction of specular reflection) by a lens and focused onto the entrance slit of a grating monochromator(f/3 Bausch & Lomb) tuned to 532 nm. The SH signal was detected with a photomultiplier

(Hamamatsu R212) and then averaged by means of a gated integrator/boxcar averager (Stanford Research Systems). The 1.064-μm fundamental frequency was eliminated from the collected radiation by a filter.

To normalize the fluctuation in laser output, a reference SH signal was generated using a 532-nm detection line from a quartz crystal, which was tuned to the peak of a Maker fringe. In addition to spectral response, the quadratic dependence of the SH signal on the incident laser power served to verify that the recorded signal was indeed SHG. Furthermore, the SH signal generated from the electrode surface due to a p-polarized fundamental was observed to be significantly greater than the SH signal arising from an s-polarized 1.064-μ beam.

Quartz Crystal Microbalance

The QCM crystals were prepared as previously described (12,21,25). Gold films of ca. 170-nm thickness were vapor deposited (Edwards E306A vacuum system) onto both sides of a planar AT-cut quartz crystal(Valpey-Fisher). A thin film(ca. 5 nm) of Si on the quartz substrate helped to improve adhesion of the gold layer on the crystal. The gold surface was cleaned electrochemically, and the quartz crystal was operated at 5 MHz. The QCM operation frequency was measured with a high precision frequency counter (Philips PM6654) to the nearest 0.1 Hz. The potentiostat and oscillator electronics have been described(25), as has the geometry of the electrode pads(8,25). The QCM electrode area in this work was 0.34 cm^2. The electrochemical cell employed was a two-compartment cell, as used previously(12), equipped with a Pt counter electrode; the reference electrode was Ag/AgCl (Microelectrodes, Inc.). Current and frequency measurements were made at 1.5 mV intervals and recorded on an IBM PC/AT.

Results and Discussion

Measurement of current, SH signal, and QCM oscillatory frequency were obtained as a function of electrode potential for sulfuric acid solutions and for copper sulfate in sulfuric acid solutions, as described in the succeeding sections. The experiments were conducted in the potential region between +0.6 V. and -0.1 V. vs Ag/AgCl. Confinement to this potential range assures no oxide formation at potentials more positive than about +0.7 V, and also prevents bulk copper electrodeposition, which occurs at potentials slightly more negative than -0.1 V.

Cyclic Voltammetry

The cyclic voltammetry obtained at an electrochemically cleaned vapor-deposited gold surface on a quartz substrate is shown in Fig. 1 for a solution of sulfuric acid. The voltammogram is essentially flat until potentials negative of about +0.2 V are reached on the cathodic sweep. The small rise in cathodic current at these potentials is presumably due to the desorption (and resulting partial charge transfer) of a small portion of an adsorbed sulfate layer on the gold surface, as determined by earlier voltammetric(26), capacitance(27), and QCM(28) measurements. These results differ slightly with those obtained in an ex situ measurement of sulfate species adsorbed on a Au(111) surface(29), wherein it is suggested that sulfate does not desorb at any potentials within the voltage range under study. Sulfate and bisulfate specific adsorption on platinum electrodes has been confirmed by previous surface sensitive IR spectroelectrochemistry experiments(30,31), and capacitance measurements on silver in sulfuric acid electrolyte(32) have shown the contact adsorption of sulfate species on this metal. The observations show that, in general, sulfate species are specifically adsorbed to the surfaces of the electrodes within the double layer po

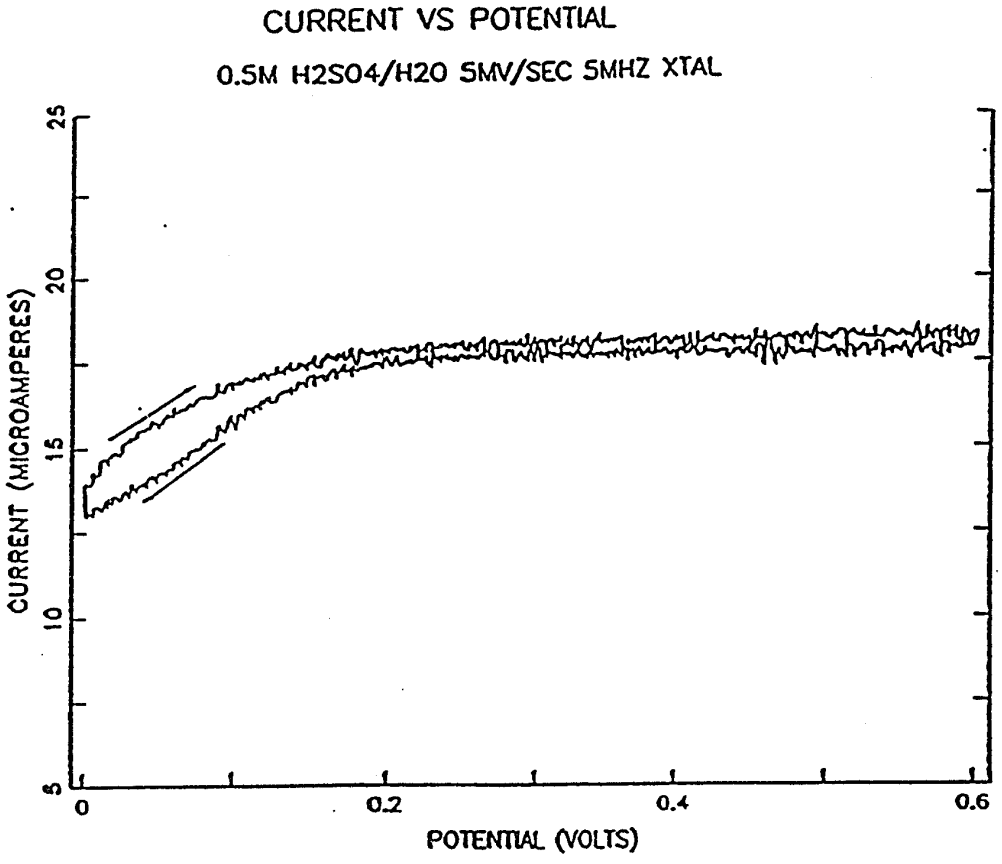

1. Cyclic voltammogram on Au of 0.5 M H_2SO_4 in H_2O; the sweep rate was 5 mV s^{-1}, and potentials are vs. the Ag/AgCl reference electrode.

tential region. (The double layer region is the voltage range in which no redox reactions occur, and the electrode is said to be ideally polarized.) This is in contrast with the case of perchlorate solutions. Perchlorate is generally regarded as a nonadsorbing ion, which results in a much narrower double layer region than that obtained in sulfate media(31,33).

The cyclic voltammogram obtained on an electrochemically cleaned vapor-deposited gold surface in solutions containing millimolar Cu(II) ion in solution(as copper sulfate) is shown in Fig. 2. Two cathodic waves are observed during the potential sweep to less positive potentials, and two corresponding anodic peaks are seen on the reverse scan. On single-crystal gold surfaces (Au{111}) these two voltametric waves are more pronounced(34). The observed voltammetry is different from that observed for copper UPD in perchlorate media(21), demonstrating the influence of coadsorbed sulfate species. The voltammetry illustrated in Fig. 2 shows that during the cathodic sweep copper UPD occurs in two stages, which contrasts with the observation in perchlorate electrolyte(21), where no well-defined UPD waves appeared. On the reverse (anodic) sweep two corresponding current peaks are observed due to the stripping of underpotentially deposited copper adlayers formed initially in the cathodic excursion. These observations are in part similar to the results obtained for the perchlorate system(21), in which significant stripping peaks were seen, one for the bulk layer and one for the UPD copper adlayer. Presently, we have no explanation for the differences in copper UPD that were seen in sulfuric acid vs perchlorate acid. It is apparent that the electrolyte employed may have a significant influence on the UPD process.

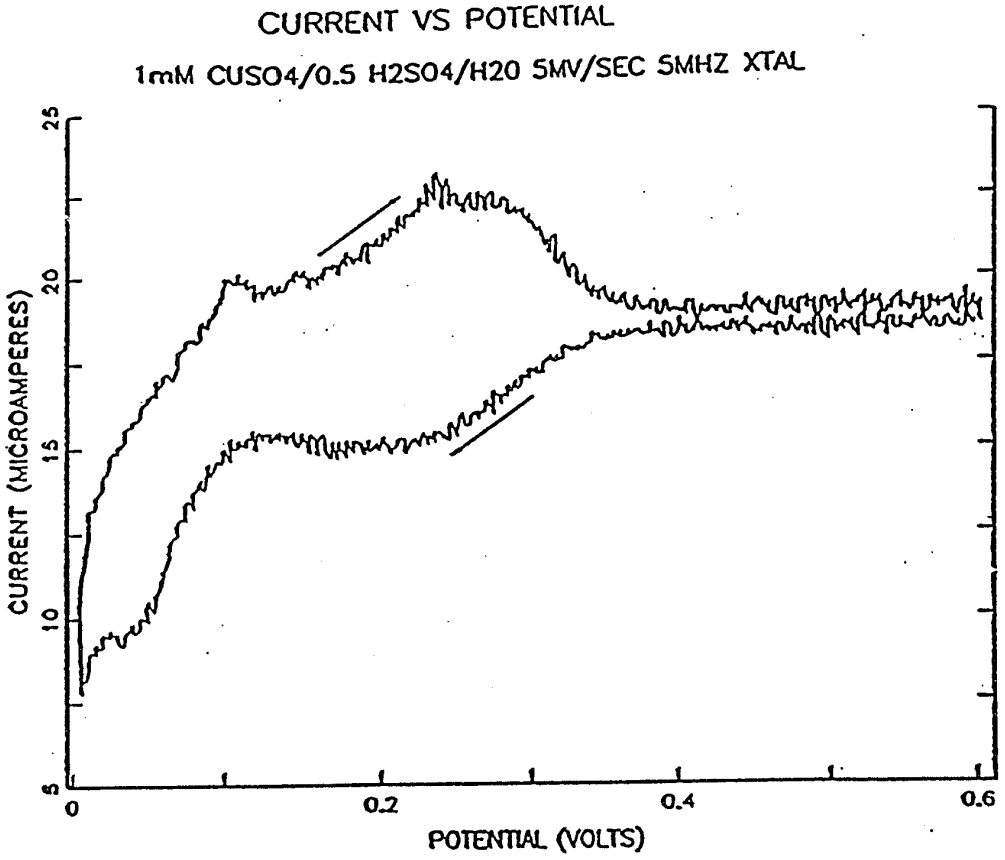

2. Cyclic voltammetry on Au of 1 mM $CuSO_4$ in 0.5 M H_2SO_4/H_2O; other parameters are as described in Figure 1.

Second Harmonic Generation

Figure 3 shows the SHG signal obtained from the gold surface as a function of potential in a sulfuric acid solution containing no dissolved copper ion. The SHG intensity is essentially constant during the oxidation-reduction cycle (ORC), in contrast with previous observations on silver(35) and platinum(36). The results in sulfuric acid are also quite different from data obtained in perchlorate electrolyte (which is weakly adsorbing) on gold surfaces(37). These results suggest that adsorbed sulfate does not become desorbed at any potential within the double layer region on gold, for a change in SH signal in this potential region might be indicative of an adsorption-desorption event(28). We anticipate that a desorption event would be accompanied by a change in SH signal, although it may be that SHG intensity changes can result from other factors besides desorption of the adsorbed sulfate. Such contentions can only be made by complementing the SHG work with other surface-sensitive techniques such as IR or QCM.

The SH signal observed during copper UPD and also during subsequent removal of copper adlayer, is shown in Fig. 4. The SHG intensity decreases substantially on the negative potential sweep, and reaches an essentially constant value at electrode potentials more negative than about +0.05 V vs Ag/AgCl. The SH signal decrease is nearly coincident with the UPD of copper on the gold surface. During the return excursion (positive potential sweep) the SH signal remains relatively constant up to a potential of approximately +0.3 V, at which point SHG increases and returns to the initial value observed prior to the negative excursion. On the return sweep the SH signal does not retrace the signal obtained during the forward sweep (Fig. 4), reflecting somewhat the separation between deposition and stripping peaks seen by cyclic voltammetry (Fig. 2). This suggests

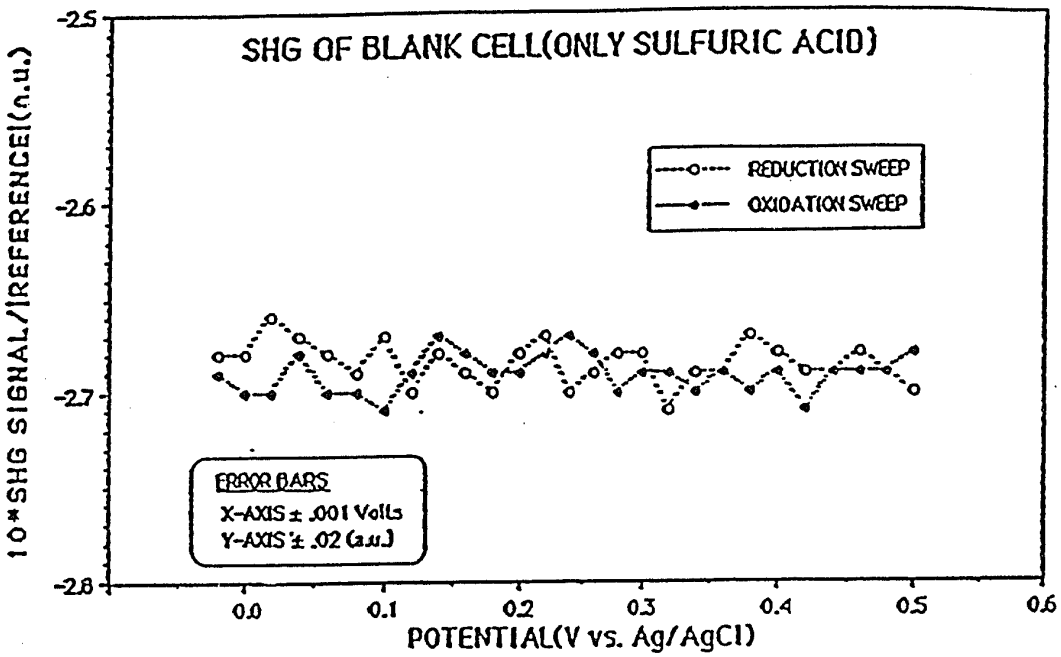

3. Plot of SHG intensity from Au against potential for the solution described in Figure 1. The error in the SHG measurement was ±2%; data were collected at static potentials.

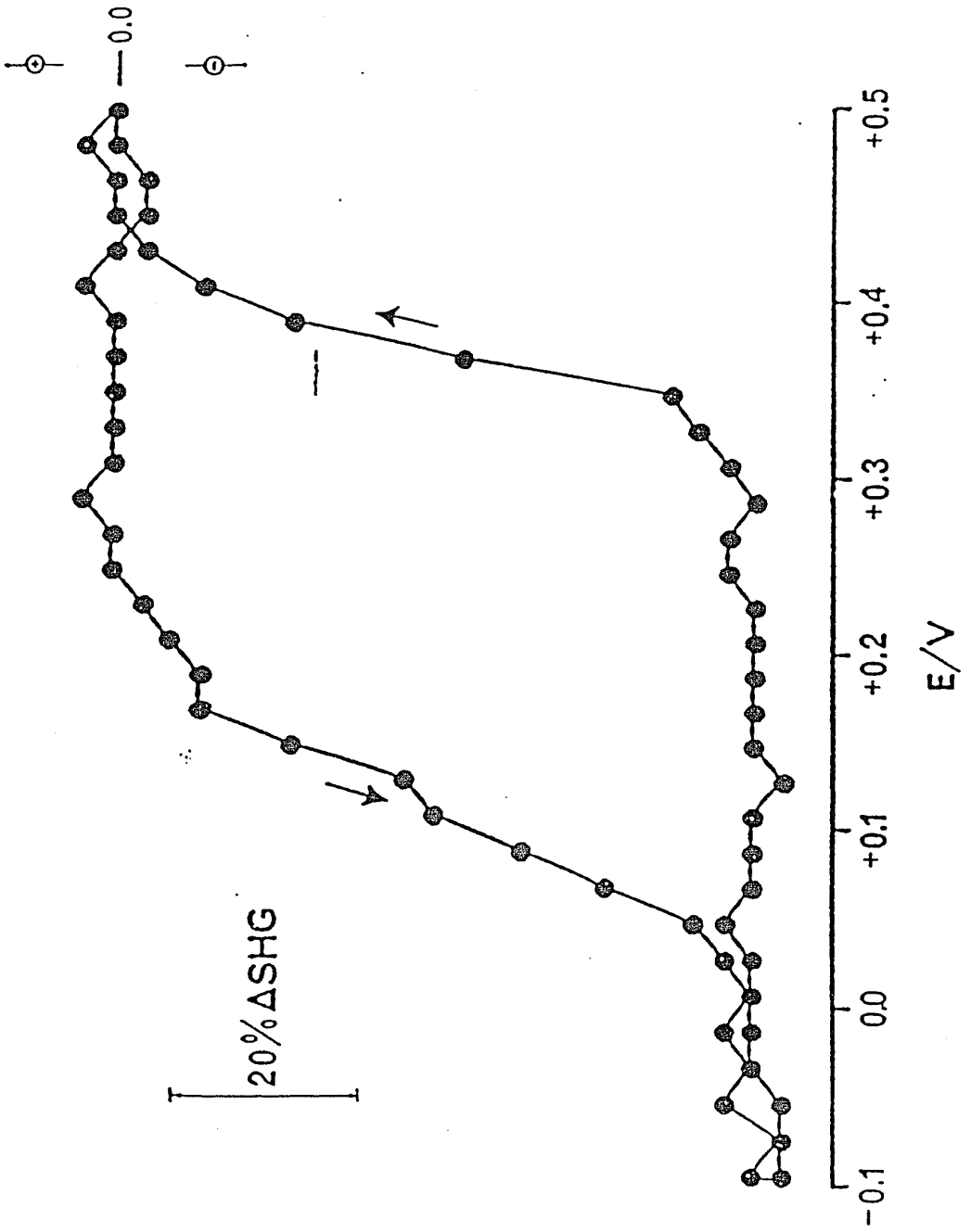

4. Measured SHG intensity vs. potential from the electrode surface for the solution described in Figure 2; other parameters are as given in Figure 3.

that significant interfacial changes occur during UPD and stripping of copper adlayers, giving rise to different potential-dependent SHG magnitudes. However, it is difficult to attribute directly the individual interfacial contributions to the SHG signal,e.g., to adsorbed sulfate, copper adlayers, the gold substrate itself, or a combination of the contributions from all three. We noted earlier that following the return (anodic) sweep the SHG detected returns to the signal intensity observed prior to the intial cathodic excursion; this indicates that the overall nature of the gold surface does not change appreciably as a result of an ORC.

The fact that the SHG signal changes substantially during copper UPD on gold shows that the optical technique is highly sensitive to underpotentially deposited submonolayer amounts of copper atoms on the gold surface. The decrease in SH intensity must arise from an overall decrease in localized electron density at the interface when copper becomes electrodeposited. On a highly crystalline gold electrode, at full coverage the adlayer copper atoms are believed to sit in three-fold hollow sites of a gold (111) surface, and the distance between copper atoms is similar to the distance between gold atoms, suggesting the formation of a 1 X 1 commensurate copper adlayer(38). Further, associated with each copper atom is an oxygen atom, the source of which is thought to be a sulfate ion(39). Thus, the copper atoms are deposited in a tetrahedral geometry, with the copper in the center, three gold atoms forming the base, and an oxygen (presumably from sulfate) at the apex of the tetrahedron. The implication is that the oxygen atoms associated with UPD copper atoms will reduce the delocalization of d-electrons of the copper adlayer, and this results in a decrease in the SH signal arising from the interface. This contention, of course, is really a plausibility argument since the gold electrode used in the experiments reported here is polycrystalline. Investigations utilizing single crystal gold surfaces of different

orientations will be valuable in elucidating the details of the morphology of metal overlayer deposition on electrodes and will be useful in comparision with other systems(19,40,41).

Quartz Crystal Microbalance

The change in QCM frequency response as a function of applied potential on a vapor-deposited gold electrode is shown in Fig. 5 for a sulfuric acid solution in which no copper species is present. We note that the gold surface in this experiment may be quite different from that in the SHG study, so only qualitative comparisons between the two experiments can be made. The slight increase in frequency (Fig. 5) that results as the potential is scanned more negatively is about an order of magnitude less than the frequency change that would be observed if sulfate species became desorbed at more negative potentials. We attribute this minimal change in frequency to sulfate/bisulfate restructuring at the gold surface as the potential is made less positive. If specifically adsorbed sulfate and/or bisulfate ions were completely desorbed at more negative potentials, a QCM frequency increase of > 10 Hz would be expected (from the Sauerbrey equation).

Figure 6 shows the observed potential-dependent frequency response of the gold-modified QCM in a coppersulfate/sulfuric acid solution. We see a substantial decrease in QCM frequency during copper UPD, which begins at a potential of about $+0.35$ V vs Ag/AgCl (coincident with the onset of cathodic current during the reductive sweep, see Fig. 2) and continues with a broad adsorption wave to approximately $+0.02$ V before bulk copper deposition occurs. This demonstrates the submonolayer sensitivity of the QCM technique. The measured QCM frequency change during the anodic stripping of the UPD copper is 9.0 ± 0.5 Hz. With an electrode area of 0.34 cm2, this frequency change corresponds

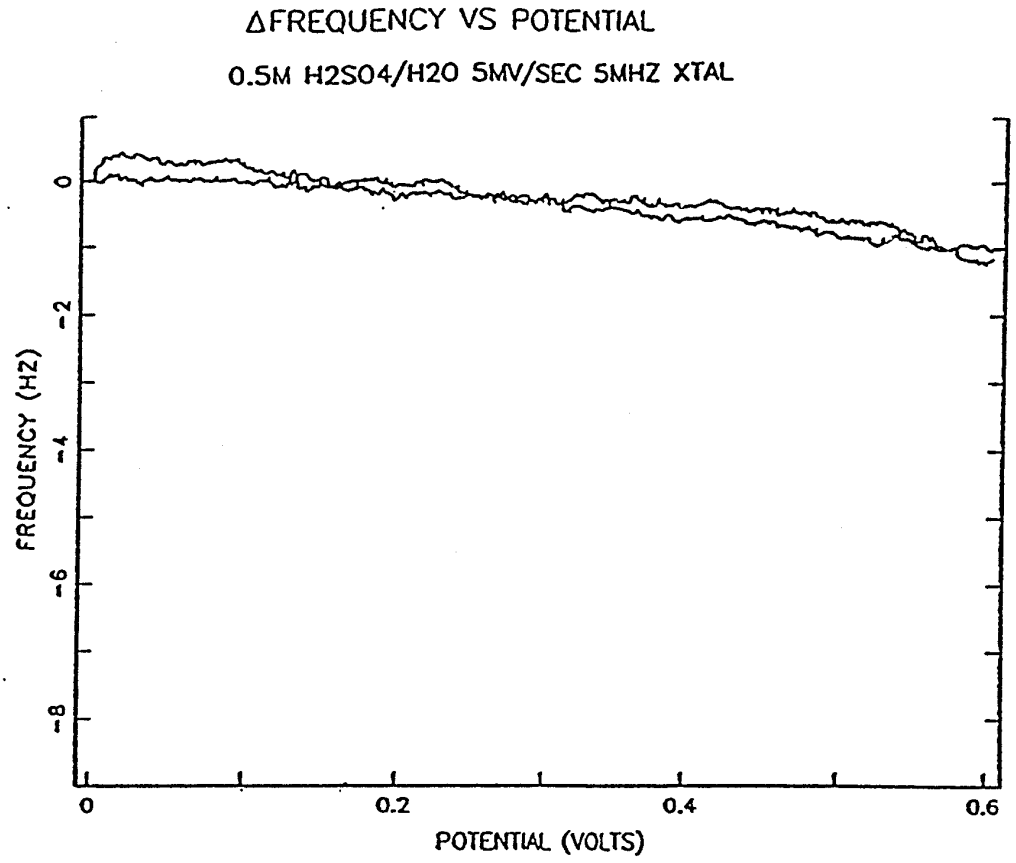

5. Response of measured Au QCM frequency vs. potential for the solution described in Figure 1. The resonator frequency was 5 Mhz; other parameters are as described in Figure 1.

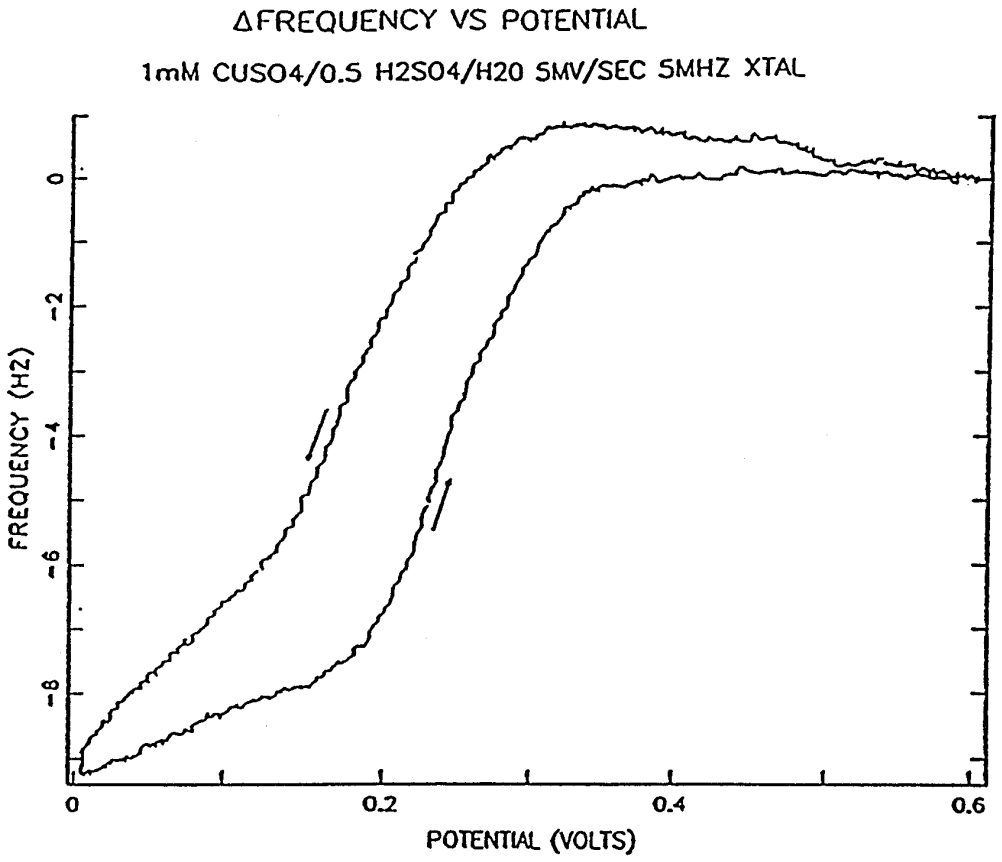

6. Plot of Au QCM frequency potential dependence (potentials vs. Ag/AgCl) for the system described in Figure 2; sweep rate and resonator parameters are as given in Figures 1 and 5, respectively.

to a mass increase (as obtained from the Sauerbrey equation) of 5.0 x 10^{-8} g/cm^2 or 8.0 x 10^{-10} mol/cm^2. For the UPD copper deposited on the gold surface, this computed coverage is approximately that calculated for copper UPD on a Au(111) surface in perchlorate electrolyte(21,42). Specific estimates for surface coverage may well be unique to the preparation and pretreatment of the gold electrode and even the electrolyte employed. The observed frequency change is comparable to the value obtained previously for copper UPD in perchlorate media(21).

From the anodic stripping charge for the underpotentially deposited copper the electrosorption valency γ is calculated from:

$$\gamma = -(dq / d\Gamma)/ F$$

where q is the charge passed per unit area during UPD (in coulombs/cm^2), Γ is the surface coverage of the UPD adlayer (in moles/cm^2), and F is the Faraday constant (96,493 coulombs/mole). The electrosorption valency is the charge required for adsorption of an underpotentially deposited ion and can vary between zero and the ionic charge. Our computed value for γ is 1.5 for UPD copper, which is comparable to values estimated by others who have examined both Cu UPD ($\gamma = 1.4$) and the Cu bulk deposition ($\gamma = 2.0$ - 2.1) for this system in perchlorate(21).

Conclusion

Optical second harmonic generation and quartz crystal microbalance techniques are used as in situ probes of copper underpotential deposition on polycrystalline gold surfaces in sulfuric acid electrolyte. The second harmonic signal from a polished bulk gold substrate is observed to decrease by >60% as

a result of copper underpotential deposition on gold. Also, the mass of an underpotentially deposited copper adlayer is monitored in situ by an oscillating quartz crystal microbalance, yielding an estimated coverage of ca. 8.0×10^{-10} mol/cm^2 and an electrosorption valency of 1.5 for a copper adlayer on the surface of vapor-deposited polycrystalline gold.

We have shown in this study that SHG and QCM methods can be used in situ to monitor submonolayer amounts of underpotentially deposited copper at gold electrode surfaces. It should be mentioned, however, that SHG alone cannot give quantitative estimates of surface coverages; rather, the SH signal must be calibrated against another surface-sensitive quantitative technique such as the electrochemical QCM. Further details concerning the surface structure of an underpotentially deposited metal layer on an electrode substrate can only be obtained at single crystal surfaces, and such efforts will be the subjects of future studies.

References

1. K. Ashley and S. Pons, **Chem Rev.** 88, (1988) 673.
2. K. Ashley, **Spectroscopy** 5, (1990) 22-32.
3. G. L. Richmond, J. M. Robinson, and V. L. Shannon, **Prog. Surf. Sci.** 28, (1988) 1-70.
4. V. L. Shannon, J. M. Robinson, and G. L. Richmond, **Spectroscopy** 3, (1988) 44-53.
5. Y. R. Shen, **Nature(London)** 337, (1989) 519-525.
6. J. H. White, M. J. Albarelli, H. D. Abruna, L. Blum, O. R. Melroy, M. G. Samant, G. L. Borges, J. G. Gordon, **J. Phys. Chem.** 92, (1988) 4432-4436.
7. R. K. Chang and T. E. Furtak, Electrochemical Effects in Surface Enhanced Raman Scattering, (Plenum, New York, 1982).
8. M. R. Deakin and D. A. Buttry, **Anal. Chem.** 61, (1989) 1147A-1154A.
9. J. H. Kaufman, K. K. Kanazawa, and G. B. Street, **Phys. Rev. Lett.** 53, (1984) 2461-2464.
10. D. Orata and D. A. Buttry, **J. Am. Chem. Soc.** 109, (1987) 3574-3581.
11. R. R. McCaffrey, S. Bruckenstein, and P. N. Pasad, **Langmuir** 2, (1986) 228-229.
12. M. R. Deakin, T. T. Li, and O. R. Melroy, **J. Electroanal. Chem.** 243, (1988) 343-350.
13. S. Bruckenstein and M Shay, **Electrochim. Acta.** 30, (1985) 1295-1300.
14. V. L. Shannon, D. A. Koos, and G. L. Richmond, **Appl. Opt.** 26, (1987) 3579-3583.
15. P. Guyot-Sionnest, W. Chen, and Y. R. Shen, **Phys. Rev. B** 33, (1986) 8254-8263.
16. P. Guyot-Sionnest and Y. R. Shen, **Phys. Rev. B** 35, (1987) 4420-4426.
17. J. E. Sipe, V. Mizrahi, and G. I. Stegeman, **Phys. Rev. B** 35, (1987) 9091-9094.
18. G. Z. Sauerbrey, **Z. Phys.** 155, (1959) 206-212.
19. D. A. Koos, **J. Electrochem. Soc.** 136, (1989) 218C-220C.
20. T. E. Furtak, J. Miragliotta, and G. M. Korenowski, **Phys. Rev. B** 35, (1987) 2569-2572.
21. M. R. Deakin and O. R. Melroy, **J. Electroanal. Chem.** 239, (1988) 321-331.

22. D. K. Roe, J. K. Sass, D. S. Bethune, and A. C. Luntz, **J. Electroanal. Chem.** 216, (1987) 293-301.

23. K. Ashley, S. Pons, **Trends Anal. Chem.** 4, (1985) 142-147.

24. M. J. Bennahmias, S. Lakkaraju, B. M. Stone, and K. Ashley, **J. Electroanal Chem.** 280, (1990) 429-434.

25. O. R. Melroy, K. K. Kanazawa, J. G. Gordon II, and D. A. Buttry, **Langmuir** 2, (1986) 697-700.

26. H. Agnerstein-Kozlowska, B. E. Conway, A. Hamelin, and L. Stoicoviciu, **Electrochim. Acta.** 31, (1986) 1051-1061.

27. A. Hamelin, T. Vitanov, E. Sevastyanov, and A. Popov, **J. Electroanal. Chem.** 145, (1983) 225-264.

28. W. Stockel and R. Schumacher, **Ber. Bunsenges. Phys. Chem.** 93, (1989) 600-605.

29. M. S. Zei, D. Scherson, G. Lempfuhl, and D. M. Kolb, **J. Electroanal. Chem.** 229, (1987) 99-105.

30. K. Kunimatsu, M. G. Samant, H. Seki, and M. R. Philpott, **J. Electroanal. Chem.** 243, (1988) 203-208.

31. K. Kunimatsu, M. G. Samant, and H. Seki, **J. Electroanal. Chem.** 258, (1989) 163-177.

32. G. Valette, **J. Electroanal. Chem.** 122, (1981) 285-297.

33. K. Ashley, M. G. Samant, H. Seki, and M. R. Philpott, **J. Electroanal. Chem.** 270, (1989) 349-364.

34. D. B. Parry and G. L. Borges; work presented at the Western Spectroscopy Association Annual Meeting, Asilomar, CA (Jan. 1990.).

35. G. L. Richmond, **Surf. Sci.** 147, (1984) 115-126.

36. D. J. Campbell and R. M. Corn, **J. Phys. Chem.** 92, (1988) 5796-5800.

37. P. Guyot-Sionnest and A. Tadjeddine, **J. Chem. Phys.** 92, (1990) 734-738.

38. O. R. Melroy, M. Samant, J. G. Gordon, L. Blum, J. H. White, M. J. Albar elli, M. Mcmillan, and H. D. Abruna, **Langmuir** 4, (1988) 728-732.

39. L. Blum, H. D. Abruna, J. H. White, J. G. Gordon II, G. L. Borges, M. G. Samant, and O. R. Melroy, **J. Chem. Phys.** 85, (1986) 6732-6738.

40. J. Miragliotta and T. E. Furtak, **Phys. Rev. B** 37, (1988) 1028-1030.

41. D. A. Koos, V. L. Shannon, and G. L. Richmond, **J. Phys. Chem.** 94, (1990) 2091-2098.

42. J. W. Schultze and D. Dickertman, **Surf. Sci.** 54, (1976) 489-505.

Chapter III. GRAZING INCIDENCE X-RAY AND ELECTROCHEMICAL STUDY OF THIN FILM COPPER(111) ON MICA

Introduction

In-situ electrochemical/interfacial studies at single crystal surfaces owe part of their success to the availability of large area, atomically smooth, high quality (i.e., highly crystalline) thin film electrodes. It has been known that a select group of substrates, such as carefully prepared mica, allow for the deposition (up to a few nm) of several metals in high vacuum, with the exposed metal surface being atomically smooth and showing a high degree of epitaxy(1). These epitaxial metal films on substrates such as mica are viable alternatives to bulk single crytal metals, which tend to be expensive and also small in size (1-2 cm^2). In addition, single crystals require careful treatment for surface preparation, for their surfaces are not guaranteed to be as pristine as those obtained by growing high quality thin films in vacuum. These advantages have led to the utilization of high quality thin film single crystals in interfacial studies of a variety of phenomena, both in-situ(2-8) and ex-situ(9-12). Since there are many possible applications for high quality single crystal thin films, we describe in this chapter the preparation and characterization of Cu(111) on mica substrates.

Both chemical and structural probes were used to characterize the vapor-deposited copper films. The structural probes employed were surface x-ray diffraction (XRD) and scanning tunneling microscopy (STM). Surface (grazing incidence) XRD was used to obtain information on the crystallinity, domain size, and mosaic spread of the crystalline domains. STM images were obtained to

check the smoothness of the prepared surface. The chemical probe used was electrochemical underpotential deposition (UPD) of metal adlayers on the as-prepared copper films. It is well established that UPD of metals on electrode surfaces is highly sensitive to the surface crystallinity of the electrode(3), among other factors (e.g., metal identity, electrolyte, solvent, etc.). Here we monitor UPD of Pb and Tl on epitaxially grown Cu on mica.

Experimental

Copper thin films were evaporated onto cleaved mica discs (Green Muscovite, ASTM V-2 or better; Ashville Schoonmaker Mica Co.) at 2 x 10^{-6} torr and 300° C. Following the cleaving step the mica substrates were rinsed with deionized (Nanopure, 18 MΩ) , organic-free (Organopure) water, and then dried at 100° C. The cleaved mica substrates and copper shot(99.999%, Aldrich) were then loaded into a cryo-pumped evaporator (Edwards model E306A), and were pumped down and outgassed at 300° C for 6-8 hours. Evaporation of copper onto the cleaved mica surface was typically done at 2-4 x 10^{-6} torr and at a rate of 10-12 Å/sec, up to a thickness of 2500 Å. Samples were subsequently cooled to room temperature in high vacuum and used immediately.

X-ray scattering data from vapor-deposited copper on mica surfaces were collected on beam line X20C at the National Synchrotron Light Source (NSLS) at Brookhaven National Laboratory, Upton, New York; the diffraction geometry employed has been described previously(13). A Si(111) double monochromator was used to tune the x-ray beam to 8046.8 eV (1.5408 Å), and the x-ray beam was focussed at the sample position. The incident beam intensity was monitored via a kapton beamsplitter and NaI scintillation detector. The diffracted x-ray beam from the sample was filtered through 1 mrad Soller slits and analyzed by

a second NaI scintillation detector, both being attached to a 4-circle diffractometer (Huber). Sample alignment was achieved by locating the bulk Cu(101)h and (011)h reflections. All data were collected in the symmetric ($\omega = 0$) mode.

The scanning tunneling microscope employed was a Nanoscope I benchtop instrument equipped with a tungsten tunnelling tip. STM scans were run in constant voltage mode at bias potential of 10 V. The tunneling dimensions (x,y,z) over the surface were 3800 x 3800 x 60 Å.

For the electrochemical experiments, a Princeton Applied Research model 173 potentiostat and model 175 waveform programmer were used in conjunction with a standard 2-compartment glass cell. Vapor-deposited copper on mica wafers were attached to one compartment of the cell via an 0-ring seal, thereby exposing the epitaxial copper surface to the solution. The counter and reference electrodes were Pt and Ag/AgCl, respectively. A glass frit separated the working and counter electrode cell compartments.

All electrolytes employed were made from high purity chemicals: Na_2SO_4, anhydrous (99+%, AESAR); $Pb(CH_3COO)_2$ (Ultrapure, Alfa); Tl_2SO_4(99.9%, Aldrich) ; CH_3COOH (Ultrapure, Alfa). Deionized H_2O (18MΩ resistivity) was employed for the preparation of all solutions, and where deoxygenation was necessary, UHP argon(99.999%) was used. All potentials are reported versus the Ag/AgCl (3M KCl saturated with AgCl) reference electrode.

Results and Discussion

Preliminary Laue and x-ray diffraction spectra of vapor-deposited copper films on mica had suggested a predominantly Cu(111) surface. Evidence of the (111) nature of the Cu surface for similarly prepared copper films has been pre-

sented previously by low energy electron diffraction (LEED) (9) and reflection high energy electron diffraction (RHEED) (10) studies. Following our preliminary Laue and XRD studies, the as-prepared copper film surfaces were analyzed by grazing incidence x-ray diffraction at the NSLS facility. Figures 1 and 2 show the results (ϕ-scan and H-scan, respectively) obtained from grazing incidence XRD off the Cu surface. The azimuthal (ϕ) scan (Figure 1) shows the mosaic spread of the Cu(111) domain is approximately 0.1° , as indicated by the full width at half maximum of the diffraction peak. The peak reveals six-fold symmetry in ϕ, indicating a hexagonally close-packed (111) surface. The radial H-scan (figure 2), which closely approximates a θ - 2 θ scan, gives information on nearest-neighbor spacings, as defined by the peak position. The parameter H is found from the figure to be 1.129 reciprocal lattice units (RLU), where 1 RLU = 2.518 $Å^{-1}$. The full width at half height of the peak in Figure 2 gives a measure of the domain size of Cu(111) surface domains. We determined a domain size of approximately 300 Å, and a d-spacing of 2.21 Å. This d-spacing yields a Cu-Cu distance of 2.55 Å, which is in agreement with the literature value for copper of 2.556 Å(14). The grazing incidence XRD data suggest that the epitaxial copper films are of very high quality (as indicated by an extremely small mosaic spread) and show substantial areas of the surface which are crystalline (111) in nature.

An STM image of the epitaxial copper surface is show in Figure 3. Although the copper surface is rougher than epitaxial gold(2) and silver(11) surfaces prepared by similar techniques, there are substantial regions of the copper surface that are atomically flat. The Cu(111) domains can be readily seen in the STM image, and the scan shows our previous estimate of domain size (on the order of 300 Å), as determined by grazing incidence XRD, is reasonable. Similar results have been obtained on specially prepared bulk copper single crystals(15,16).

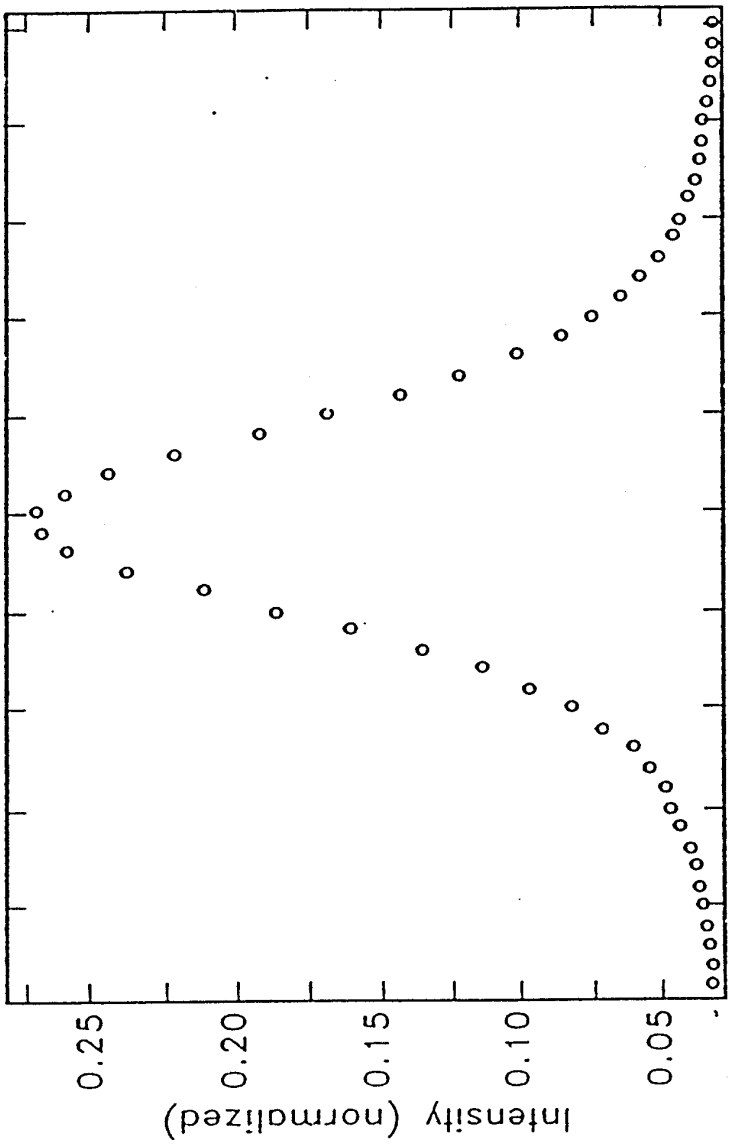

Figure 1. Phi scan from grazing incidence XRD of 2500Å Cu(111) film on Mica.

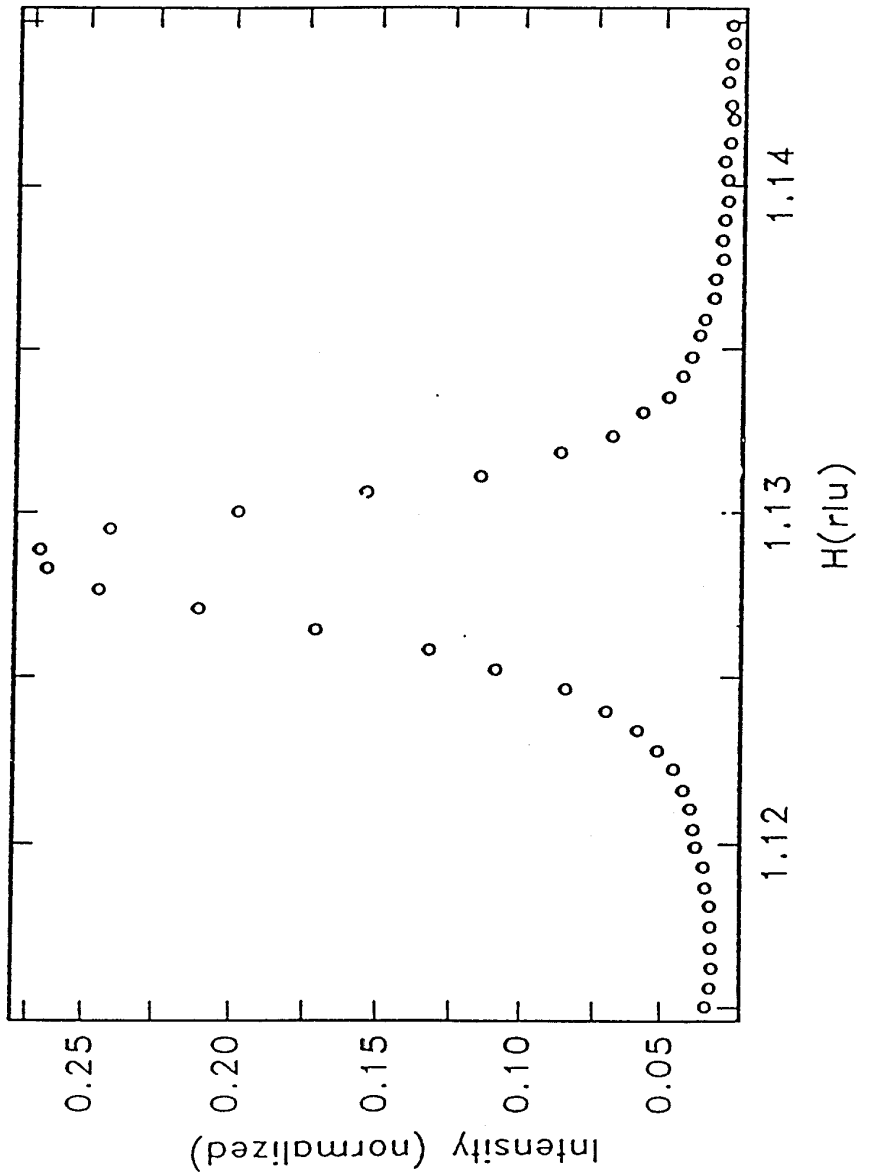

Figure 2. H scan from grazing incidenc XRD of 2500Å Cu(111) film on Mica.

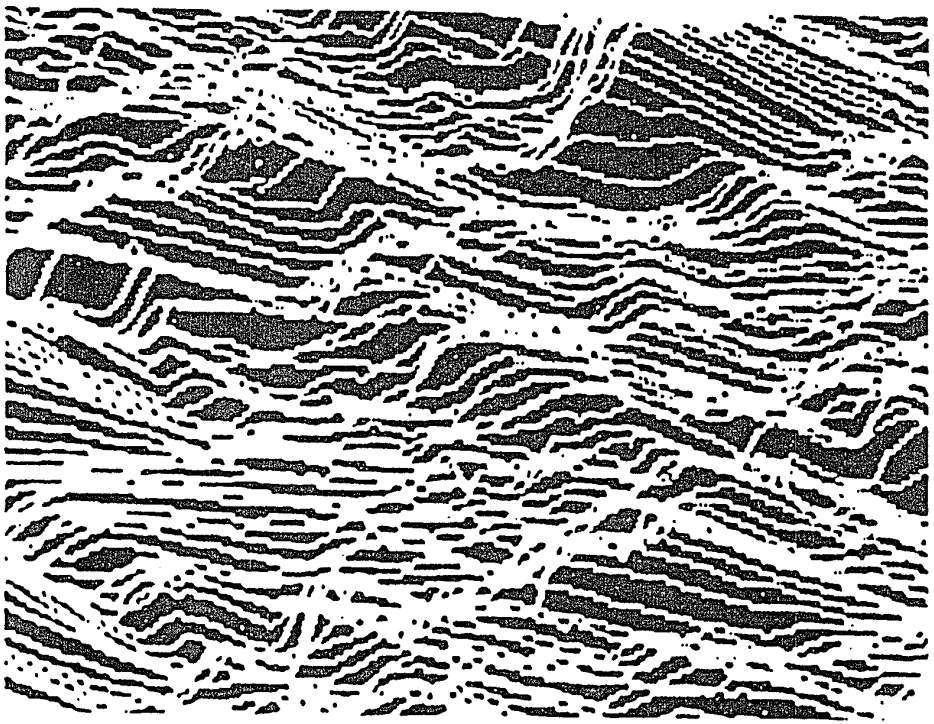

Figure 3: 1000Åx1000Å STM Image of 2500Å Cu(111) film on Mica; 60Å Resolution. Tunsten Tunneling Tip; $V_{tip}=10\,mV$; $I_{tip}=0.1\,nA$.

Figure 4 shows a cyclic voltammogram obtained during the underpotential deposition (UPD) of Pb (as the acetate dissovled in acetate electrolyte) onto a vapor-deposited Cu film. The results are essentially identical to those obtained for this system at the same sweep rate on bulk Cu(111) surfaces(4,5). A sharp deposition peak(-.545 V.), attributed to the formation of a lead monolayer, is observed during the negative sweep. The sharpness of the deposition peak is due to the formation of a lead monolayer of highly ordered structure. Such a feature would not be seen on rougher surfaces; rather, the UPD peak would be much more rounded, lacking fine structure(17).

On the return scan the stripping peak is somewhat less sharp, and the peak potential is shifted ca. 60 mV with respect to the deposition peak potential. At slower scan rates this peak separation is decreased. A small shoulder also appears on the UPD stripping peak, which is indicative of some surface roughening (recall figure 3). The potential shift between the deposition and stripping peaks has been shown to be a funciton of the supporting electrolyte(5), as well as scan rate. Once formed, the UPD adlayer becomes thermodynamically stabilized as a result of surface adsorption of ions and orientation of solvent molecules. An "overpotential" of sorts must then be applied to the return scan, so that the energy required to strip off the UPD adlayer may overcome the stabilization energy of the surface layer of electrolyte and/or solvent. Indeed, it has been shown for similar systems that it may be necessary to expel anions from the surface during UPD and subsequent stripping of UPD adlayers(18,19). This effect can cause peak separations (between deposition and stripping peaks) such as that observed in the cyclic voltammogram of the lead UPD on Cu(111) system(Figure 4). There is evidence that UPD metal monolayers are polarized compared to analogous bulk metal

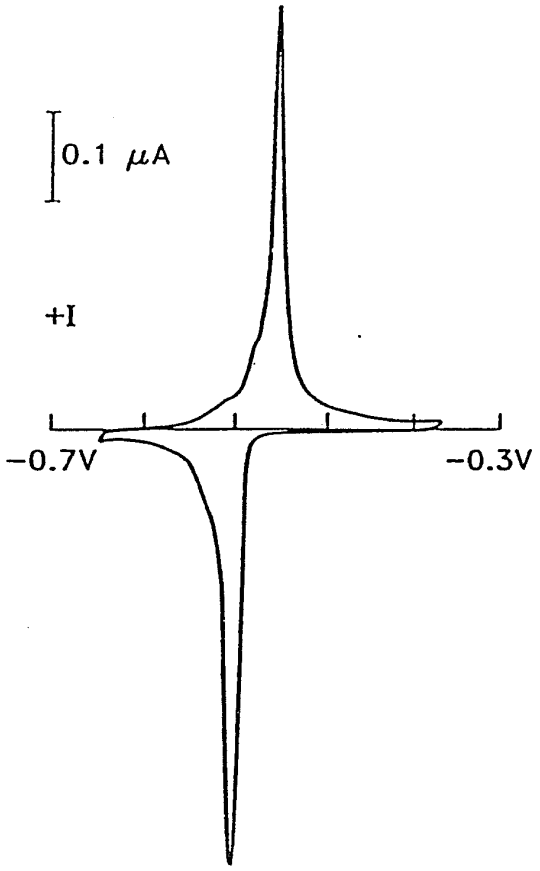

Figure 4. Underpotential deposition of Pb on to Cu(111)/mica electrode. Electrolyte: 5mM $Pb(CH_3COO)_2$ in 0.5M $NaCH_3COO$/0.1M CH_3COOH Scan Rate: 5 mV/sec.

species(3), so that additional ionic stabilization of the UPD adlayer would result whether the adlayer is fully discharged or not.

By measuring the charge passed during UPD of lead, we obtained a lead monolayer coverage of 335 $\mu C/cm^2$, which is comparable to the value of 320 $\mu C/cm^2$ determined previously on bulk Cu(111)(5). This charge is also close to the theoretical value of 310 $\mu C/cm^2$ (assuming full discharge of the lead UPD adlayer(20)), which is expected for a close packed Pb monolayer on a Cu(111) surface(4,21).

Figure 5 shows the voltammetry observed during UPD of thallium onto vapor-deposited Cu film. In this case two UPD peaks(-.435 V. and -.725 V.) are seen, and they are attributed to the deposition of two successive Tl monolayers onto the Cu surface. There are peak shifts between deposition and stripping peaks for both waves, the first wave (peak separation approx. 100 mV) showing the greatest irreversibility of the two. The irreversibilities exhibited in the Tl UPD voltammograms are thought to be due to similiar thermodynamic and kinetic effects as described above for Pb. The fact that the second UPD wave shows less peak separation than the first is possibly due to the change in work function difference between the two layers concerned(3). The differences in work function between a Tl monolayer and the Cu substrate is greater than the work function difference between a second Tl layer and another Tl monolayer below it. This leads to a stabilization effect which scales to the UPD shift of the monolayer in question. Hence less "stripping overpotential" is required to remove the second Tl UPD layer from the first Tl monolayer, compared to removal of the first Tl UPD layer from the Cu substrate. This results in a greater peak separation (between deposition and stripping peaks) for the first Tl UPD wave than for the second(Figure 5). Similar results have been obtained previously on Ag(111)(22)

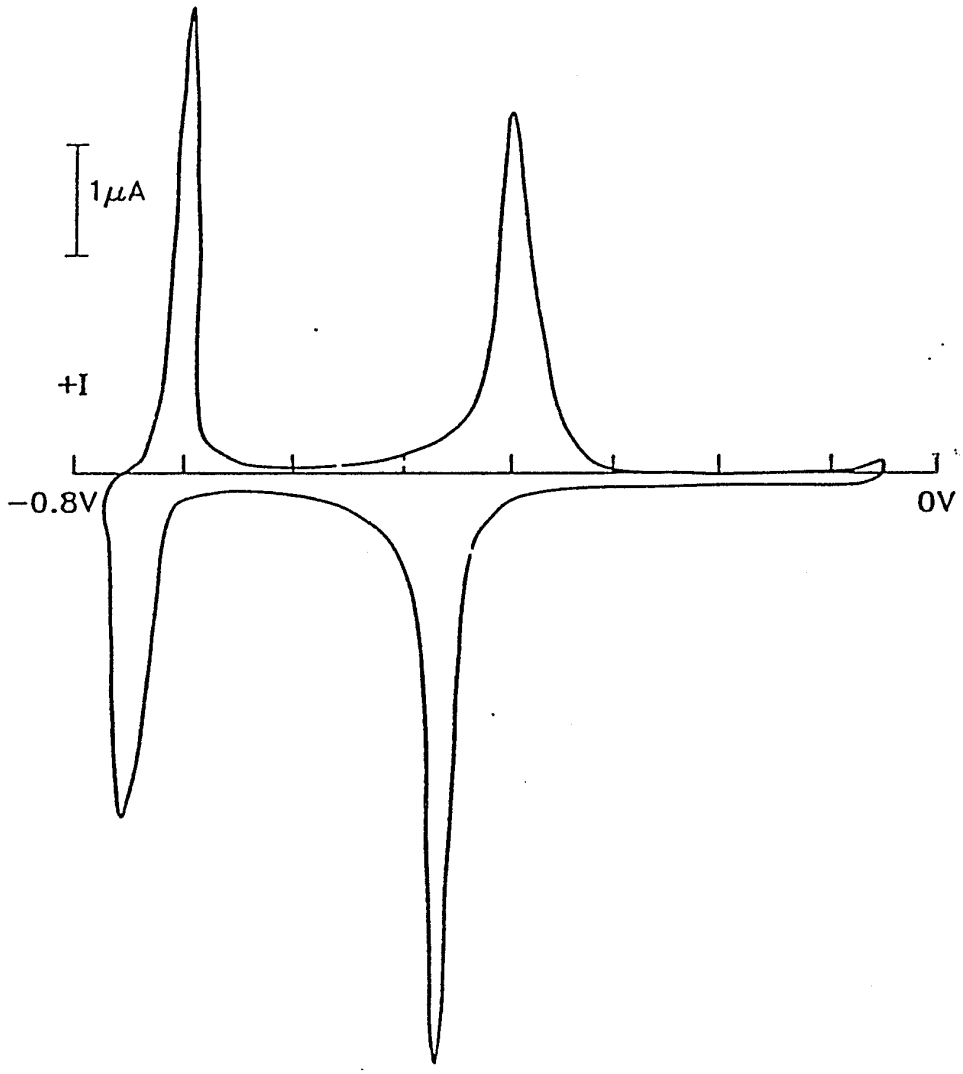

Figure 5. Underpotential deposition of Tl on to Cu(111)/mica electrode.
Electrolyte: 2.5mM T12S04 in 0.5M Na2S04
Reference Electrode: Ag/AgCl
Scan Rate: 20 mV/sec.

and Cu(111)(23) surfaces. We also note that our voltammetric results illustrate a higher degree of order than previous studies on a bulk Cu(111) surface(23), as indicated by the much sharper UPD peaks seen in this work (Figure 5). This suggests that the surface of the vapor-deposited Cu film has smaller defect density than the Cu surface prepared from bulk copper single crystals.

The total charge measured during Tl UPD was found to be 350 $\mu C/cm^2$, which contrasts with the value for a Tl hexagonally close-packed monolayer of 160 $\mu C/cm^2$(22). While there is no literature value for UPD Tl on vapor-deposited Cu(111) available, Tl UPD on Ag(111) shows similar voltammetry, and coverages of 380 $\mu C/cm^2$ have been measured for bulk crystal Cu(111)(22) and 320 $\mu C/cm^2$ for Ag(111) on mica(24). These coverages for Tl UPD on Ag(111) and our value for Tl UPD on vapor-deposited Cu(111) are then higher than the modeled coverages for a simple hexagonally close-packed monolayer of Tl. Furthermore, it has been determined by grazing incidence x-ray scattering that the UPD of Tl on Ag(111) includes the formation of a monolayer in the first set of adsorption peaks, with the formation of a bilayer upon the appearance of the second set of adsorption peaks(24). Our measurements for the first adsorption peaks for Tl UPD on vapor-deposited Cu(111) on mica yields a value of 220 $\mu C/cm^2$, which is more than enough charge to account for a Tl monolayer. This strongly suggests that Tl UPD on Cu(111) is also a system where both UPD monolayer and bilayer are formed prior to bulk Tl deposition. Additionally, the sharpness of the Tl UPD peaks suggests a high degree of surface order.

Conclusion

The preparation of evaporated thin films of largely single crystalline copper on mica substrates is reported. Most of the exposed copper surface has (111) ori-

entation, as established by grazing incidence x-ray scattering and electrochemical studies. The (111) surface domains are on the order of 300 Å in diameter and have a mosaic spread of ca. 0.1 °. Underpotential deposition (UPD) shifts for Pb and Tl on these Cu(111) films are approximately 150 and 300 mV, respectively. Tl is shown to form a UPD bilayer on this substrate. These epitaxial Cu films can be utilized in electrochemical surface/interface studies.

In summary, electrochemical and grazing incidence x-ray diffraction studies of vapor-deposited copper films indicate a predominance of (111) nature at the surface. We propose the vapor deposition process outlined in this chapter as a method for preparing high quality epitaxial Cu films. Such surfaces are extremely useful for in-situ studies of the electrode-solution interface.

References

1. E. Grunbaum, Epitaxial Growth; Academic Press: New York, 1975; Ch. 9.

2. E. Holland-Moritz, J. G. Gordon II, G. L. Borges, and R. Sonnenfeld, **Langmuir** 7 , 301 (1991).

3. D. M. Kolb, M. Przasnyski, and H. Gerischer, **J. Electroanal. Chem.** 54 , 25 (1974).

4. A. Bewick, J. Jovicevic, and B. Thomas, **Faraday Symp. Chem. Soc.** 12 , 24 (1977).

5. J. R. Vilche and K. Juttner, **Electrochim. Acta** 32 , 1567 (1987).

6. H. Y. Lui, F. R. F. Fan, and A. J. Bard, **J. Electrochem. Soc.** 132 , 2666 (1985).

7. M. G. Samant, M. F. Toney, G. L. Borges, L. Blum, and O. R. Melroy, **Surf. Sci.** 193 , L29 (1988).

8. R. Sonnenfeld, J. Schneir, and P. K. Hansma, in Modern Aspects of Electrochemistry , Vol. 21; R. E. White, J. O'M. Bockris, and B. E. Conway, Eds. Plenum: New York, 1990; Ch. 1, and references therein.

9. S. Nagashima and I. Ogura, **Appl. Surf. Sci.** 33/34, 450 (1988).

10. M. B. Stiddard, **Thin Solid Films** 94, 1 (1982).

11. V. M. Hallmark, S. Chiang, J. F. Rabolt, and R. J. Wilson, **Phys. Rev. Lett.** 59, 2879 (1987).

12. M. Barkai, E. Grunbaum, and G. Deutscher, **Thin Solid Films** 90, 85 (1982).

13. M. G. Samant, M. F. Toney, G. L. Borges, L. Blum, and O. R. Melroy, **J. Phys. Chem.** 92, 220 (1988).

14. B. D. Cullity, Elements of X-Ray Diffraction Addison-Wesley: Reading, MA, 1984; p. 506.

15. A. Brodde, S. Tosch, and H. Neddermeyer, **J. Microsc.** 152, 441 (1988).

16. A. Samsavar, E. S. Hirschorn, T. Miller, F. M. Leibsle, J. A. Eades, and T. C. Chiang, **Phys. Rev. Lett.** 65, 1607 (1990).

17. S. Lakkaraju, M. J. Bennahmias, G. L. Borges, J. G. Gordon, M. Lazaga, B. M. Stone, and K. Ashley, **Appl. Optics** 29, 4943 (1990).

18. M. Hepel and S. Bruckenstein, **Electrochim. Acta.** 34, 1499 (1989).

19. M. Hepel, K. Kanige, and S. Bruckenstein, **Langmuir** 6, 1063 (1990).

20. M. R. Deakin and O. R. Melroy, **J. Electroanal. Chem.** 163, 327 (1988).

21. H. Seigenthaler and K Juttner, **J. Electroanal. Chem.** 163, 327 (1984).

22. M. F. Toney, J. G. Gordon II, M. G. Samant, G. L. Borges, O. R. Melroy, L. S. Kau, D. G. Weisler, D. Yee, and L. B. Sorensen, **Phys. Rev. B** 42, 5594 (1990).

23. G. Materlik, J. Zegenhagen, and W. Uelhoff, **Phys. Rev. B** 32, 5502 (1985).

24. A. T. Hubbard, **Acc. Chem. Res.** 13, 177 (1980).

IV. AN IN-SITU ELECTROCHEMICAL QUARTZ CRYSTAL MICROBALALNCE STUDY OF THE UNDERPOTENTIAL DEPOSITION OF COPPER ON AU(111) ELECTRODES

Introduction

Interfacial electrochemical studies of the solid-liquid interface are fundamentally important contributions to the science of electrochemistry. Through these interfacial studies we seek a better understanding of basic electrochemical phenomena taking place at the electrode-electrolyte interface. Interfacial (double layer) charging, electron transfer, adsorption/ desorption of species, and surface(electrode) roughening are fundamental topics still being investigated by electrochemists hoping for a better understanding of the thermodynamic and kinetic phenomena at interfaces. Although standard electrochemical techniques have provided the bulk of information from which electrochemical knowledge has risen, it has been an innovative combination of surface sensitive techniques and electrochemical methods which have shown promise for impacting electrochemical knowledge. The innovations of spectroelectrochemistry, where UV-Vis(1), IR(2), Surface Enhanced Raman(3), or Second Harmonic Generation(SHG)(4) were done, and also X-ray fluorescence(5) and scattering(6), etc., when applied to electrochemical investigations, have proven to be very successful for providing unique insights into interfacial phenomena. More recently, scanning tunneling microscopy(STM) has been applied in-situ, to probe the electrochemical interface(7). Each combination of in-situ techniques brought with it some unique contribution or application to interfacial electrochemistry. However, many times these combinations also brought their own unique re-

quirements or limitations. No particular combination of electrochemistry and in-situ surface sensitive probe has proven to be the panacea of knowledge to interfacial electrochemistry. It is the clever combination of electrochemistry and another in-situ surface sensitive probe which has provided an innovative approach to electrochemical interfacial studies.

Another unique combination of electrochemistry and an in-situ, surface sensitive probe is the quartz crystal microbalance(QCM). The first electrochemists to incorporate the QCM in liquid media combined mass analysis and cyclic voltammetry to measure the interfacial events occurring on the electrode surface(8). The QCM, as applied to electrochemical systems, was found to be capable of detecting monolayer changes in mass. Kanazawa and coworkers described the QCM response to mass changes in liquids with the Sauerbrey relation(9):

$$\Delta f = -2\Delta m\, n\, f_o^{\,2} / (A(\mu_q \rho_q)^{1/2})$$

and found the QCM to behave predictably when rigid layer conditions were applied uniformly to electrode surfaces(10). Here, Δf is the change in oscillator frequency, Δm is the change in interfacial mass, n is the overtone number(equal to unity for this work), f_o is the QCM fundamental frequency(10 Mhz for this work), A is the unit area of the oscillator, μ_q is the shear modulus of quartz(2.947x1011 g/cm s^2), and ρ_q is the density of quartz(2.648 g/cm^3).

The combination of the QCM with electrochemical techniques has enabled researchers to measure mass changes accompanying electrode processes for electroplating and film growth(11), oxide growth and reduction(12), ion uptake into polymeric films(13), monolayer and submonolayer deposition(UPD) of

metals(8), and weak adsorption from ions in solution(14). The high sensitivity to mass changes at the electrode surface for the QCM has provided the electrochemist with valuable interfacial information which is very difficult to determine by other means.

This work employs both electrochemistry and the QCM techniques and is further enhanced by the use of crystalline gold electrodes: Au(111). It has been known for some time that several metals can be grown in thin film crystalline form(15). It has also been shown that electrochemical interfacial processes are very sensitive to the electrode crystallinity(16). Use of a crystalline electrode (where the electrode's atomic structure is initially known) for interfacial studies is a much more fundamental approach to investigating interfacial changes. Crystalline electrodes have been employed in-situ, under potentiostatic control by several groups using x-rays(4,5), optical techniques(17), and even by STM microprobe techniques(7). This work is a unique demonstration of Cu UPD in H_2SO_4 on what is seen by electrochemistry to be a Au(111) electrode which has been incorporated into the QCM.

Experimental

Quartz Crystal Oscillators(QCM) used were 1 inch diameter AT-Cut quartz operated at 10 MHz and polished to an optical finish on both sides(Valpey-Fisher). Gold electrodes were vapor-deposited onto both sides of the quartz crystal microbalance as described earlier(18) with the following enhancement. The air electrodes were vapor-deposited first with 50 Å of Cr to enhance adhesion, followed by gold depositon to a thickness of 2500 Å. Evaporation conditions were 5×10^{-6} torr vacuum, at a rate of 1-2 Å/sec for Cr and 8-12 Å/sec for gold at room temperature. Gold working electrodes were

vapor-deposited onto the uncoated side of the QCM at 300 ° C in a vacuum of 2–6 x 10^{-6} torr at rates of 8–12 Å/sec to a final thickness of 2500 Å. This procedure produced Au working electrodes of high (111) quality. All Au(111) electrodes were used immediately after cooling to room temperature under vacuum.

Cyclic voltammograms were run on a homemade potentiostat which is interfaced to the QCM oscillator circuitry, as described previously(8). Voltammograms were initiated and digitized on an IBM XT equipped with an IBM data aquistion card. The electrochemical /QCM cell is shown in Figure 1. The function of this cell allows stress-free mounting of the QCM crystal to a simple 2–compartment electrochemical cell employing counter electrode, reference electrode, and deoxygenating bubbler. The QCM/Electrochemical cell was set up in a sheilded box which provided protection from external RFI/EMI noise and allowed for argon purging.

For these experiments all electrolytes used were made from high purity chemicals: H_2SO_4 (double distilled from vycor, GFS Chemicals); $CuSO_4$(99.999%, Alfa/Johnson Matthey). Deionized H_2O(Nanopure, Sybron/Barnstead) was used in the preparation of all electrolytes. Where deoxygenation was needed, UHP argon(99.999%) was used. All potentials are measured versus a Ag/AgCl(3M KCl saturated with AgCl) reference electrode. To minimize Cl contamination the reference electrode employed a double junction design(Microelectrodes, Inc.). All experiments were run at room temperature.

Results

Cu UPD on Au(111)

The cyclic voltammetry/QCM scan for Copper UPD in in sulfuric acid on thin film Au(111) is shown in Figure 2(solid line). Starting the voltammetry at +0.8

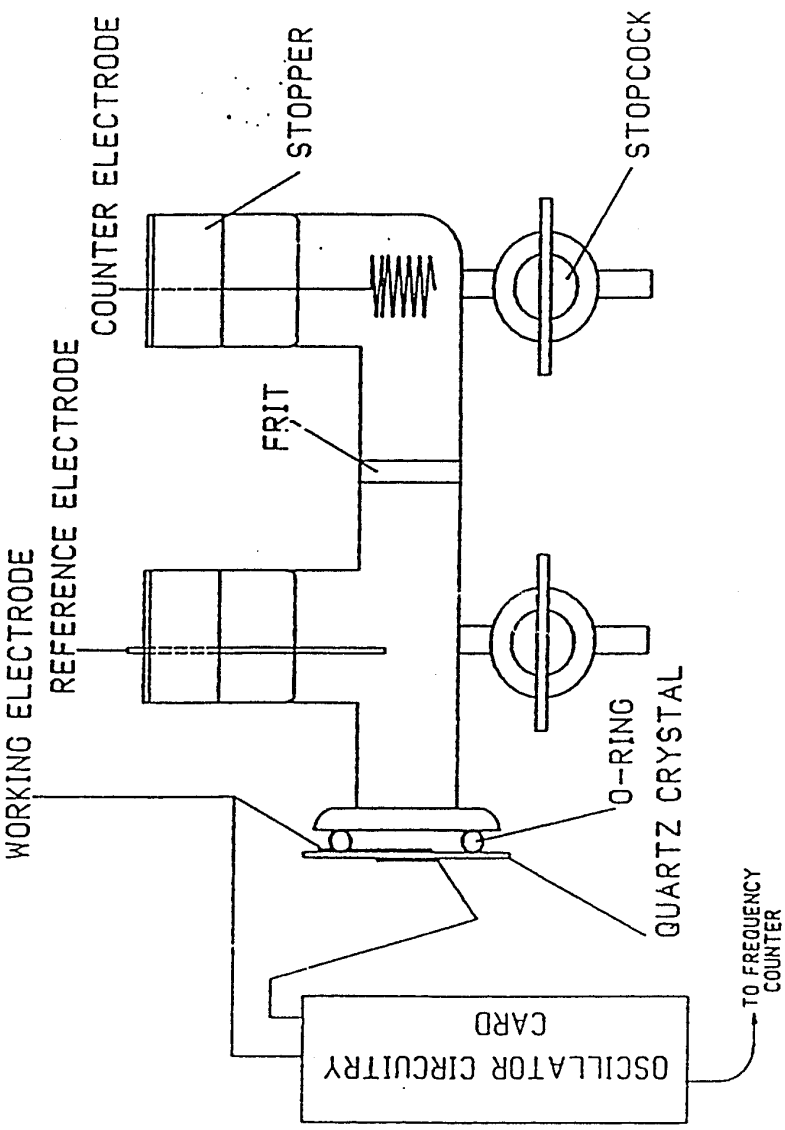

Figure 1: Schematic of glass Electrochemical/Quartz Crystal Microbalace Cell.

V(vs. Ag/AgCl) and scanning the potential on the thin film Au(111) electrode negative, the first UPD reduction peak appears at +0.28 V, followed by a second reduction peak at +0.08 V. Upon reversing the scan UPD copper is reoxidized in two waves at +0.13 V and +0.30 V. Scanning more negative than -0.10 V yields bulk copper deposition on gold. The data shown in Figure 2 are very similar to the characteristic cyclic voltammetry reported by Itaya(19), Kolb(20,21), and others for copper UPD in sulfuric acid on a single crystal Au(111) electrode. The charge collected for copper UPD is 470 μ/cm^2 and compares quite well with the calculated charge value of 445 μ/cm^2 for a copper monolayer epitaxial to the Au(111) lattice. For a 2 electron reduction of copper, it is believed that 445 μ/cm^2 corresponds to a monolayer of copper having been uniformly deposited onto the Au(111) electrode surface(19). This conclusion of copper UPD monolayer coverage has also been drawn by others using other surface sensitive techniques,e.g. Surface Extended X-ray Absorption Fine Structure (SEXAFS) of Cu UPD on Au(111)/mica electrodes(5).

To further confirm the electrochemistry for copper UPD on thin film Au(111) as being nearly identical to Cu UPD on single crystal Au(111), a comparison of Cu UPD on both thin film and bulk single crystal Au(111) is shown in Figure 3. Allowing for the differing sizes between the two Au(111) electrodes and a slight voltage difference between reference electrodes used in each experiment, it is clear that the thin film Au electrode on the QCM is largely (111) in nature, as determined by electrochemistry. An estimate of the roughness for the electrode used in Figure 1 which is based upon the Copper UPD charge yields a value of 1.07. A perfectly smooth electrode surface would have a roughness factor of 1.0. This roughness factor of 1.07 compares well with other values obtained for single

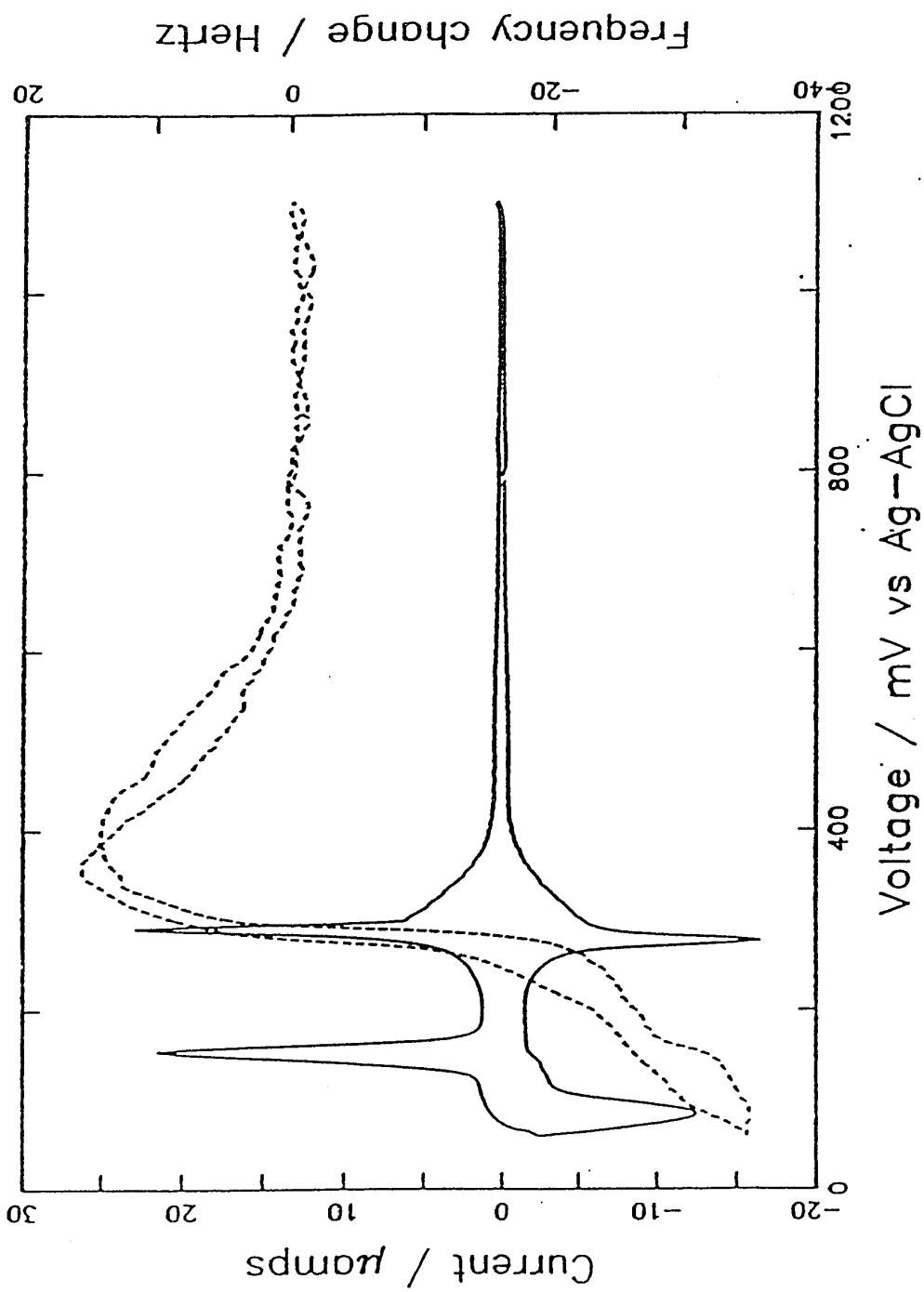

Figure 2: Copper UPD on thin film Au(111)/QCM(solid), QCM response(dashed). 2.5 mM $CuSO_4$ in 0.1 M H_2SO_4; scan rate is 10 mV/sec.

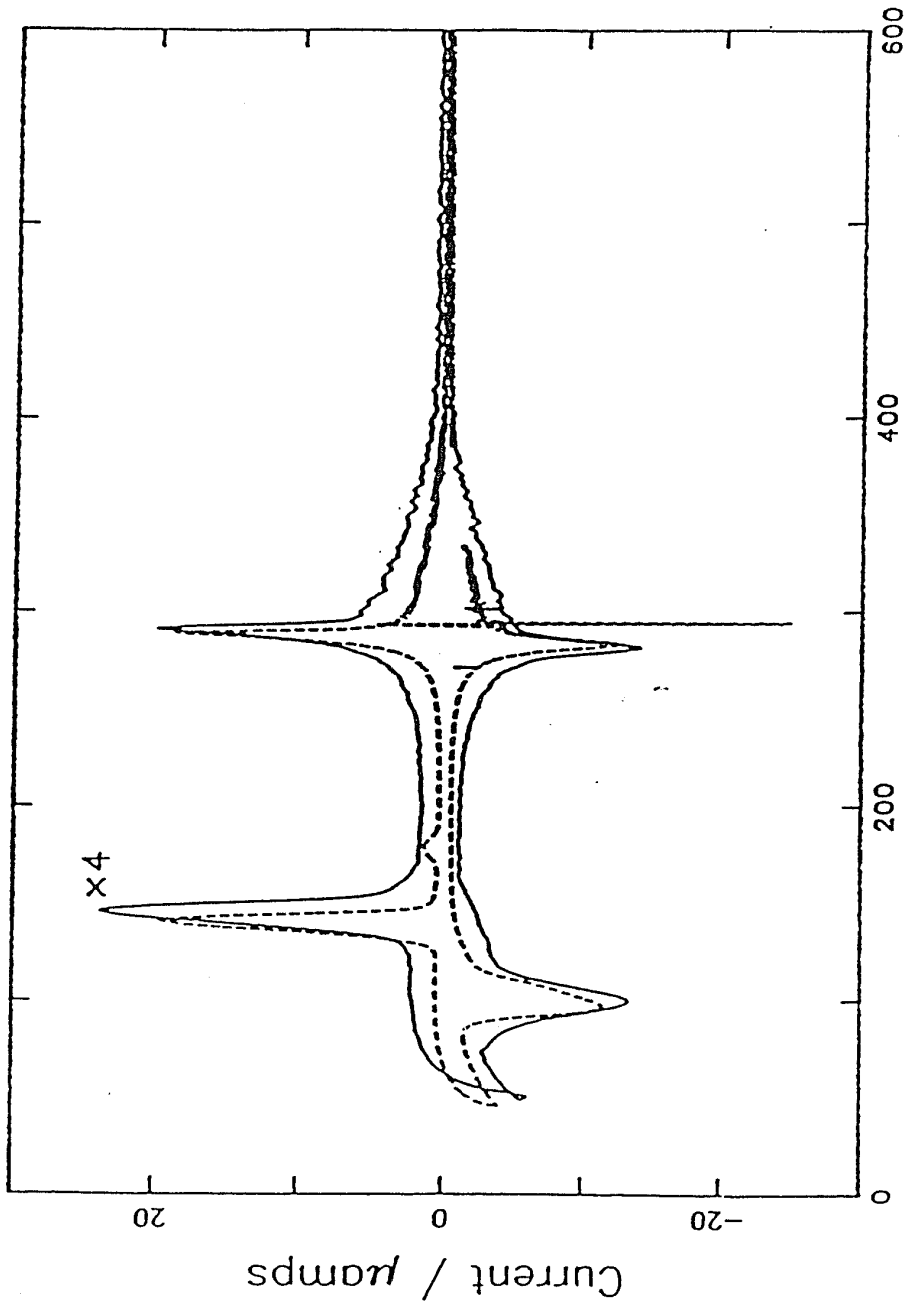

Figure 3: Copper UPD on thin film Au(111) (solid) and on Single Crystal Au(111) (dashed). 2.5 mM $CuSO_4$ in 0.1 M H_2SO_4; scan rate is 2 mV/sec. Voltammograms are scaled and corrected for reference electrode differences.

crystals and is considered to be a rather smooth electrode (22). Apparently, smoothness correlates with (111) quality for these thin film Au electrodes.

The in-situ QCM response to the copper UPD on Au(111) electrochemistry is also shown in Figure 2(dashed line). Starting at +0.8 V and scanning negative, the QCM frequency increases and then quickly decreases in unison with copper reduction which is shown in the voltammogram. Recalling the Sauerbrey relationship which describes the QCM response, a rise in frequency indicates a loss of mass at the QCM Au(111) electrode until the start of Cu reduction, where decreasing frequency indicates an increase in mass. The mass changes detected by the QCM at the electrode surface proceed reversibly during and after copper UPD. For potentials positive of +0.8 V the QCM frequency change is near zero and the current shown in the voltammogram is largely double layer charging.

From the mass and size of the copper adatom and the epitaxy of the copper monolayer on a Au(111) lattice, Melroy calculates a copper monolayer coverage of 2.3×10^{-9} mol/cm^2(23). For the Sauerbrey equation this corresponds to a frequency change for the mass of the copper monolayer of approximately 33 Hz. From Figure 2, the copper UPD begins at +0.40 V ending at +0.05 V and the QCM response is a change in frequency of 55 Hz. Clearly the QCM response for the copper UPD shown in Figure 2 includes more than the simple copper monolayer mass change(33Hz). Apparently the QCM is responding to interfacial events not observed in the electrochemistry of the copper system. For example, the increase in frequency between +0.7 and +0.4 Volts just prior to copper UPD suggests a loss of mass at the interface. Concurrently there is little or no faradaic current associated with this frequency increase until copper UPD begins(+0.44 V) and the frequency begins to fall. It is suspected that perhaps the sulfate anion

is taking part in the interfacial frequency(mass) changes during Cu UPD on the Au(111)/QCM. From electrochemical(24) and spectroelectrochemical(25) results, it is known that sulfate and bisulfate anions adsorb on Au electrode surfaces. The next experiments examine the activity of sulfate ion on the Au(111)/QCM electrode.

Sulfate on Au(111)

To further investigate this frequency change occurring just before copper UPD and to determine whether or not the copper in solution plays a role, experiments were done in sulfate electrolyte without copper in solution. Figure 4 shows the voltammetry/QCM response for sulfuric acid on the thin film Au(111) electrode. Again a frequency change appears at approximately the same potential (+.70 V) as the copper UPD experiments(Fig. 2). The QCM has detected an interfacial change occurring near +0.70 V, which is interrupted by copper UPD when copper is present in solution(Fig. 2). The overall frequency change for the sulfuric acid scans in Figure 4 is 45 Hz. If this response was due to the adsorption/desorption of surface sulfate, for the removal of a sulfate monolayer on the Au(111) surface (where one sulfate and one copper atom is shared by three gold atoms(4)), a 17 Hz frequency change is expected based on the Sauerbrey Eqn. This is what is measured in figure 2, where the electrode smoothness is very good($\simeq$18 Hz). However, the frequency change found in sulfuric acid (fig. 4, no copper present) is more than double this value.

From the voltammetry of the sulfuric acid scans(Fig. 4, no copper present) something more than the simple double layer charging is seen from the current sweep. For sulfuric acid on thin film Au(111), the voltammogram(Fig. 4) shows a doubling of current between +0.25 V and +0.70 V, which appears as a bulge

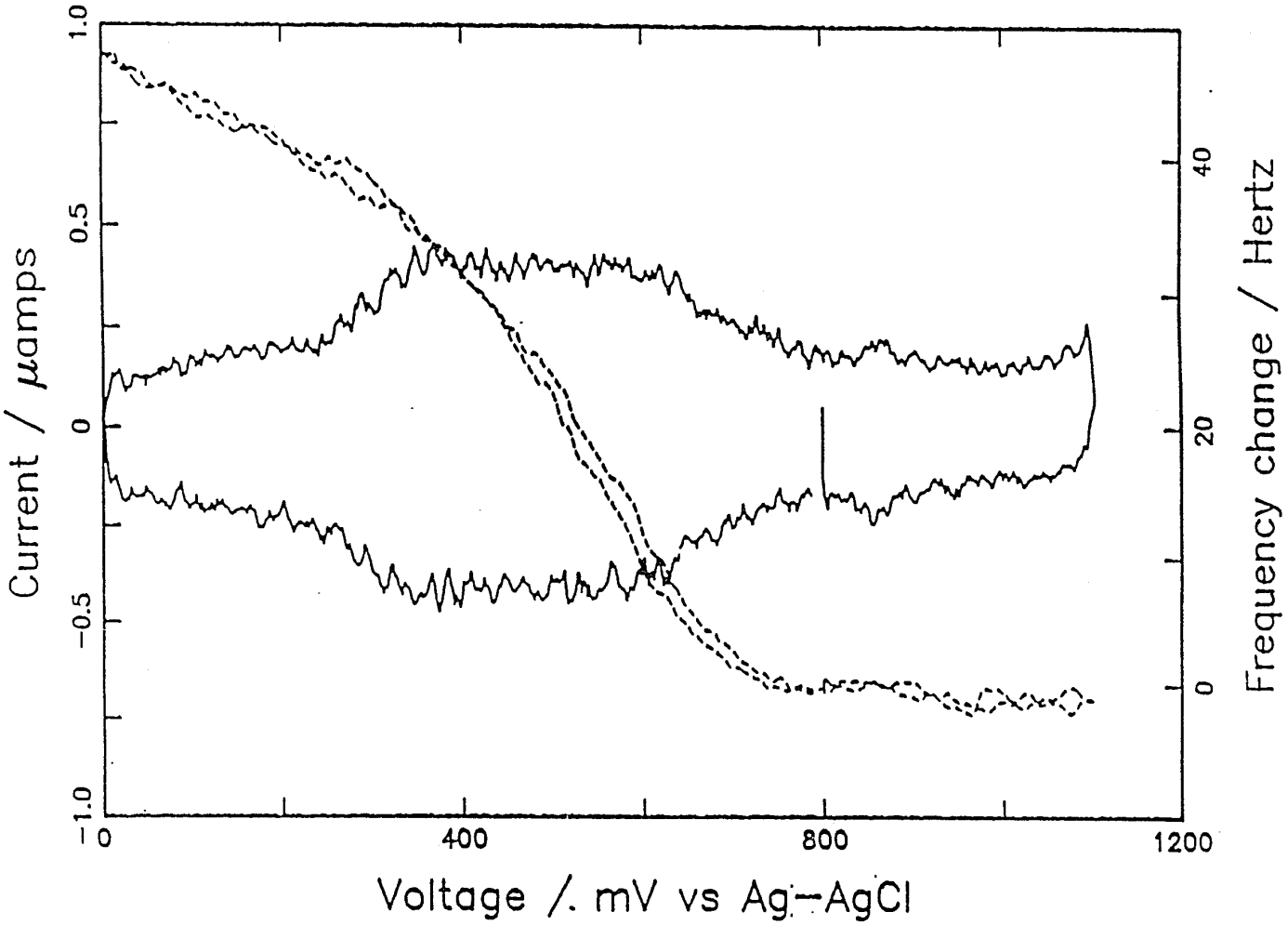

Figure 4: Cyclic voltammetry for thin film Au(111)/ QCM in 0.1 M H_2SO_4 (solid), QCM response (dashed). Scan rate is 10 mV/sec.

superimposed onto the double layer charging current. This current has been seen by Hamelin for sulfate on single crystal Au(111) electrodes and is postulated to be partial charge transfer for the weakly adsorbing sulfate anion(24). This partial charge transfer(pseudocapacitance) is a non-conventional faradaic process measured by Parsons(26) using AC voltammetry for the acetate anion adsorbing on Ag(111). The onset of partial charge transfer for the sulfate anion at +0.7 V coincides with the QCM initial frequency changes for this system. This suggests that the frequency response from the QCM is related to the interfacial changes involving surface sulfate. The frequency response for the QCM continues beyond sulfate anion charge transfer(+0.25 V) and is much too large to be accounted for by the charge passed during sulfate anion partial charge transfer.

Au(111) Oxide

As a test of the QCM response and to further demonstrate the (111) quality of the thin film Au electrode and to measure any inherent roughness, a scan of the Au oxide formation and reduction is shown in Figure 5. The Au oxide in sulfuric acid has a characteristic (111) peak (which is absent in polycrystalline gold) at +1.3 V.(24), followed by the Burhstein minima at +1.4 V(27). The number of electrons transfered per gold atom for the oxidation/reduction is electrochemically measured to be 2.0±0.2 electrons/Au atom. This compares with 2 electrons/Au atom for polycrystalline gold in perchloric acid on the QCM as measured by Bruckenstein(28). The QCM response to Au oxide formation begins at +0.9 V(Fig. 5) with a net frequency change of 8 Hz. This compares quite well to the calculated value of 9 Hz for oxide formation/reduction. From the oxide scan the thin film roughness factor is 1.3, which indicates that these

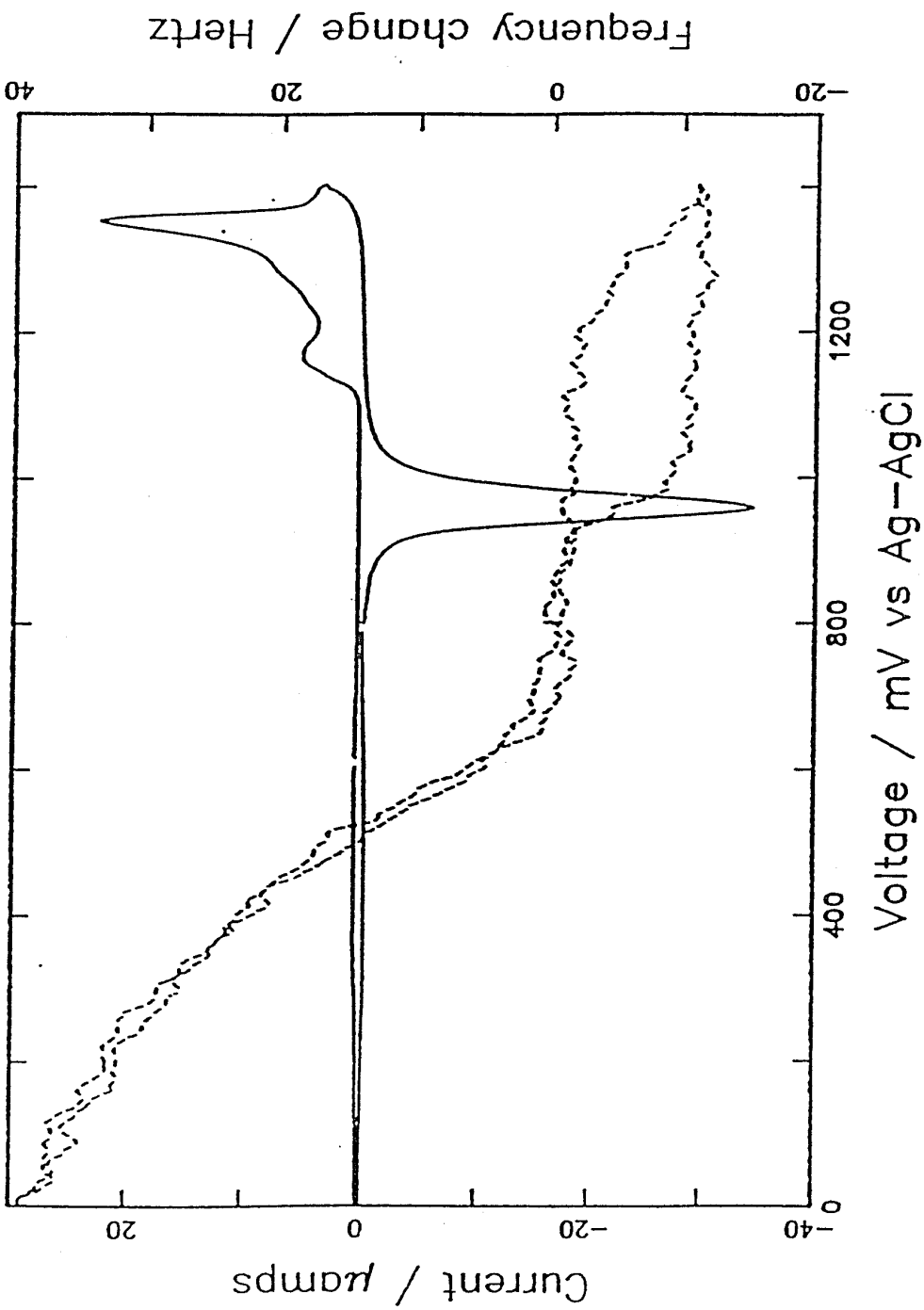

Figure 5: Thin film Au(111) oxide in 0.1 M H_2SO_4 (solid), QCM response(dashed). Scan rate is 10 mV/sec.

electrodes are roughened somewhat. The Au oxide scans demonstrate again that the thin film Au electrode is largely (111) and the QCM/voltammetry is running properly, e.g., the thin film gold working electrode is still intact on the oscillating microbalance. The substantial frequency change measured at +0.70 V in sulfuric acid(Fig. 4) truly has associated with it only a small electrochemical counterpart, the partial charge transfer for surface bound sulfate.

Sulfate and Cu UPD on Au(111)

The next experiments performed are shown in Figure 6, where the QCM/voltammetry is done first in sulfuric acid, and subsequently copper ion is added to solution(as $CuSO_4$). The QCM response shows the frequency change seen earlier for sulfuric acid(Fig. 4) with the frequency change for copper UPD(Fig. 2) neatly falling into place on the subsequent scan. This demonstrates that the sulfuric acid QCM response is indeed perturbed by the presence of copper UPD.

Discussion

The sequence of events for Cu UPD on these Au(111) electrodes as measured by the QCM describes the removal of surface ions prior to Cu UPD, with the subsequent deposition of Cu during the UPD proccess. Upon stripping of the UPD monolayer, the process proceeds reversibly. From Figure 1, where a full monolayer of UPD copper is measured (470 $\mu C/cm^2$) and the electrode is believed to be smooth(roughness = 1.07) and largely crystalline (111), a full monolayer of sulfate(18Hz) is removed from the Au(111) surface, and then the copper

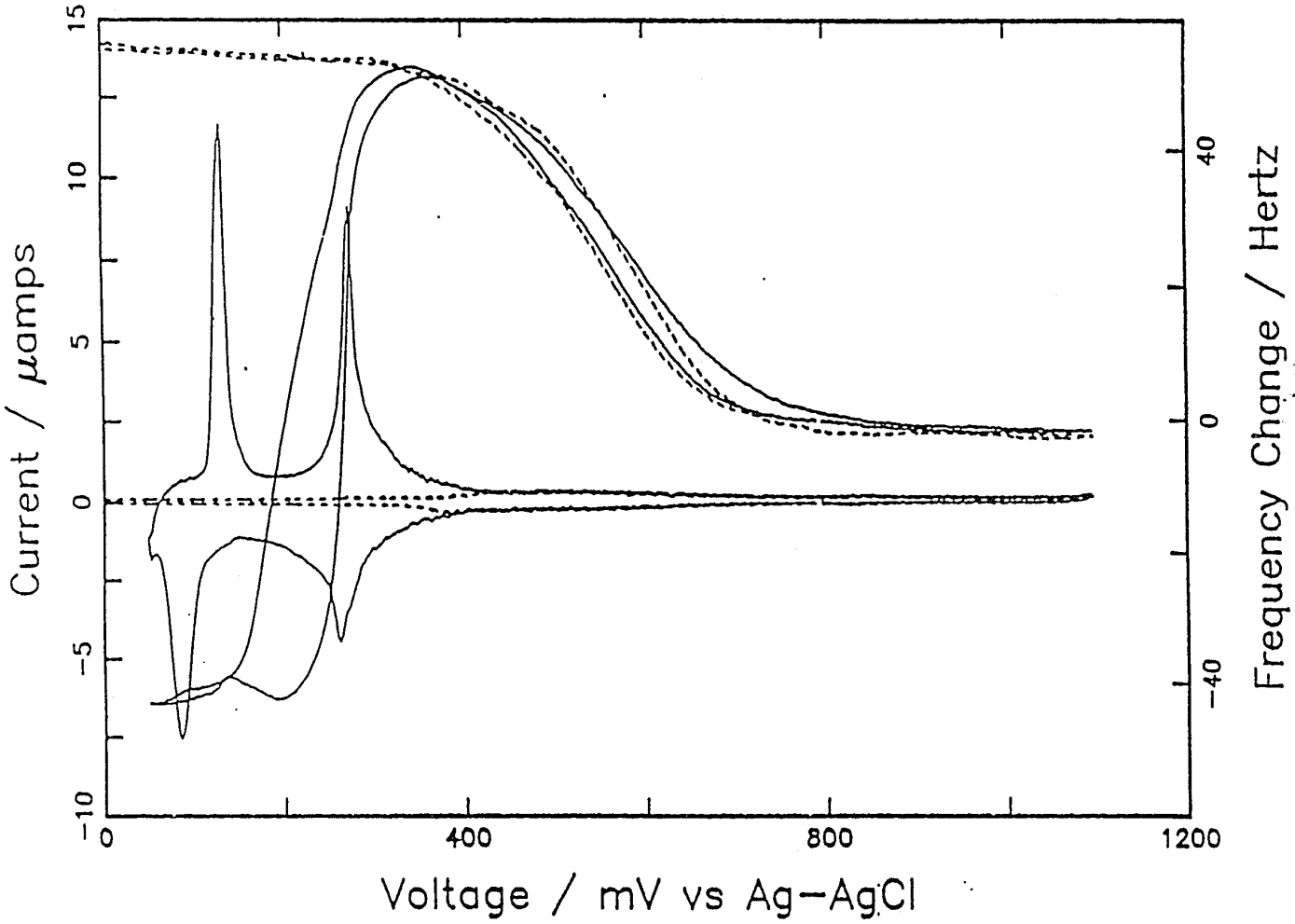

Figure 6: Voltammetry of 0.1 M H_2SO_4 on thin film Au(111)/QCM and QCM response (dashed). Excess $CuSO_4$ added (solid). Scan rate is 10 mV/sec.

monolayer is deposited along with a monolayer's worth of sulfate. It is reasonable to assume that the frequency increase prior to Cu UPD is the removal of surface bound sulfate. Experiments without Cu, i.e. sulfuric acid only, also show the removal of surface sulfate at the same potential(.75 V.). Since there is little evidence for reconstruction of the Au(111) surface in this potential range(29), the removal of surface sulfate prior to Cu UPD is a very reasonable assumption.

The total frequency change(53 Hz) for Cu UPD includes the Cu monolayer(33Hz), and associated with this monolayer, a full monolayer(17Hz) of sulfate. This also is a very reasonable description since both SEXAFS(5) and FTIR(25) see what is believed to be sulfate associated with the Cu monolayer. From Melroy's earlier work(23) on the QCM for Cu deposition on polycrystalline gold, an electrosorption valency of 1.8(and not 2) was determined for the copper deposit. This leaves a residual positive charge which could account for the sulfate anion presence.

So the proposed model for the interfacial events occuring on the Au(111) surface, as measured by the QCM and by voltammetry starts with the removal of a monolayer's worth of sulfate prior to Cu UPD, at .40 V., followed by a monolayer of Cu with one sulfate per Cu adatom being deposited, to full monolayer coverage at 0.05 V. Accounting for the roughness of the electrode(1.07), the following frequency changes(mass changes) are accounted for by this model:

Sulfate Desorption(between .75 V. and .40 V.):

$$(1.07)(17.0\ \text{Hz}) = 18.2\ \text{Hz}$$

Cu UPD and Sulfate Adsorbtion(from .40 V. to .05 V.):

$$(1.07)(33.0\ \text{Hz}) + (1.07)(17.0\ \text{Hz}) = 53.5\ \text{Hz}$$

These calculated frequency changes(18.2 and 53.5 Hz) compare quite well with the measured values of 18 Hz and 53 Hz found in Figure 1.

To complete the picture for the Cu UPD/SO_4 system on these Au(111) electrodes, a consideration of the inherent electrode roughness, an artifact of the thin film growth process must be mentioned. Not all Au(111) electrodes are as smooth as the example given in Figure 1. There is an inherent surface roughness which does appear to different extents, from batch to batch. This inherent electrode roughness is seen in Figures 4, 5, and 6 where sulfate desorption is noticeably greater than one monolayer. For example, Figure 4 shows a 55 Hz change, or 2 1/2 monolayers of sulfate. Apparently this inherent roughness does not significantly perturb the shape of the Cu UPD voltammetry as shown in Figure 6. Recalling that the Cu adatom is very sensitive to the crystal orientation of the electrode(16), for these rougher electrodes the shape of the voltammogram is largely unchanged(Fig. 6), and so non-(111) sites appear to be unavailable to Cu UPD. However, this inherent roughness does manifest itself by giving large sulfate frequency(mass) changes which diminish to 20 Hz or so, after 4-6 hours of cycling. This time dependence is not unusual, the continuous adsorption/desorption of material can smooth(provided no alloying occurs) and clean off the electrode surface. The large excess of sulfate anion present on these rough electrodes is not unheard of either. Surface Enhanced Raman Spectroscopy(SERS,(30)) is an example where upon roughening the electrode surface(by repeated ORCs), an enormous enhancement of signal for the surface species is seen.

For a roughened electrode(Fig. 6), an accounting of the interfacial frequency(mass) changes can be done, based upon the model for the Cu UPD/SO_4 system described above.

$$\Delta f_{\text{Cu UPD}} + \Delta f_{\text{sulfate}} + \Delta f_{\text{roughness}} = \Delta F_{\text{Total}} = 85 \text{ Hz.}$$

Where $\Delta f_{\text{Cu UPD}}$ is the UPD monolayer at 33 Hz, $\Delta f_{\text{sulfate}}$ is the sulfate monolayer associated with the Cu UPD monolayer at 17 Hz, and the inherent roughness is accounted for by $\Delta f_{\text{roughness}}$. $\Delta f_{\text{roughness}}$ is determined by the initial sulfate frequency increase seen prior to Cu UPD(55 Hz in Figure 6) less the sulfate associated with Cu UPD(17 Hz). Using all of these values gives a total frequency change of 88 Hz, which compares quite well with the experimental value of 85 Hz for the experiment described in Figure 6.

$$33 \text{ Hz} + 17 \text{ Hz} + (55 - 17) \text{ Hz} = 88 \text{ Hz}$$

For the case described initially, where the electrode is smooth(Fig. 1), $\Delta f_{\text{roughness}}$ is essentially zero, and all that is detected by the QCM is the release of the sulfate monolayer on the (111) surface, which is followed by the deposition of the Cu monolayer and the return of the sulfate monolayer.

Conclusion

From the voltammetry, copper UPD on these thin film Au electrodes evaporated onto the electrochemical QCM shows them to be largely crystalline (111). The total charge passed for copper UPD in sulfuric acid on these thin film Au(111) electrodes is 470 $\mu C/ cm^2$, which compares well with the literature value(20). In sulfuric acid(no copper) a current bulge is seen between +0.25 V and +0.80 V and is attributed to the weak adsorption/desorption of surface

bound sulfate anion, which appears to undergo partial charge transfer to the Au electrode. Au oxide scans in sulfuric acid(no copper) gives a charge transfer of 2.0 $\pm$0.2 electrons per gold atom, which compares with 2.0 electrons per gold atom for polycrystalline gold in $HClO_4$, and is consistent with literature values(28).

The evaporation of Au thin films onto QCM crystals at high temperatures results in largely crystalline gold (111) electrodes which is determined electrochemically by Cu UPD in sulfuric acid. This is a unique demonstration of the electrochemical QCM being fitted with a single crystal electrode on quartz. These crystalline QCM electrodes detect the desorption of a monolayer's worth of surface bound sulfate anion from the Au(111) surface prior to copper deposition(UPD). Copper UPD, as measured by the QCM, appears to be a full epitaxial monolayer of copper, with a co-adsorped monolayer of sulfate anion. As an interfacial probe, the in-situ electrochemical/QCM has demonstrated its high sensitivity to monolayer(and submonolayer) amounts of adsorbates, and provides a description of the interfacial events occuring for the Cu UPD/sulfuric acid system on Au(111).

References

1. W. R. Heineman, F. M. Hawkridge, and H. N. Blount, in **Electroanalytical Chemistry**, Vol. 13; A. J. Bard(ed.). Dekker, New York, 1974, and references therein.

2. K. Ashley and S. Pons, **Chem Rev.** 88, (1988) 673-695.

3. R. K. Chang and T. E. Furtak(eds.), in **Surface Enhanced Raman Scattering**, Plenum Press, New York, 1982.

4. G. L. Richmond, J. M. Robinson, and V. L. Shannon, **Prog. Surf. Sci.** 28, (1988) 1-70.

5. L. Blum, H. D. Abruna, J. White, J. G. Gordon, G. L. Borges, M. Samant,and O. R. Melroy, **J. Chem. Phys.** 85, no. 11 (1986) 6732-7.

6. M. G. Samant, M. F. Toney, G. L. Borges, L. Blum, O. R. Melroy, **J. Phys. Chem.** 92, (1988) 220-5.

7. R. Sonnenfeld, J. Schneir, P. K. Hansma, in **Modern Aspects of Electrochemistry**, R. E. White, J. Bockris, B. E. Conway(eds.), Plenum Press, New York, 1990; Vol. 21.

8. O. R. Melroy, K. K. Kanazawa, J. G. Gordon, and D. Buttry, **Langmuir** 2, (1986) 697-700.

9. G. Z. Sauerbrey, **Z. Phys.** 155, (1959) 206-212.

10. C. E. Reed, K. K. Kanazawa, and J. H. Kaufman, **J. Appl. Phys.** 68, (1990) 1993-2001.

11. W. D. Hinsberg, C. G. Wilson, and K. K. Kanazawa, **J. Electrochem. Soc.** 133, (1986) 1448-1451.

12. M. R. Deakin, O. R. Melroy, **J. Electrochem. Soc.** 136, (1989) 349-352.

13. J. H. Kaufman, K. K. Kanazawa, and G. B.Street, **Phys. Rev. Lett.** 53, (1984) 2461-2464.

14. M. Hepel, K. Kanige, S. Bruckenstein, **J. Electroanal. Chem.** 266, (1989) 409-421.

15. E. Grunbaum, **Epitaxial Growth**, Academic Press, New York, 1975, Ch. 9.

16. D. M. Kolb, in **Advances in Electrochemistry and Electrochemical Engineering**, , Vol. 11, Ch. 2, P. Delahay(ed.), J. Wiley & Sons, New York, 1977.

17. D. M. Kolb, in ;.bf ssb11;Spectroelectrochemistry;.pf;, R. J. Gale(ed.), J. Wiley & Sons, New York, 1988, and references therein.

18. M. R. Deakin and D. A. Buttry, **Anal. Chem.** 61, (1989) 1147-1154.

19. T. Hachiya, H. Honbo, and K. Itaya, **J. Electroanal. Chem.** 315, (1991) 275-291.

20. D. M. Kolb, **Ber. Bunsenges. Phys. Chem.** 92, (1988) 1175.

21. D. M. Kolb, **Z. Phys. Chem. N. F.** 154, (1987) 179.

22. A. Bewick and B. Thomas, **J. Electroanal. Chem.** 65, (1975) 911-931.

23. Mark R. Deakin and O. R. Melroy, **J. Electroanal. Chem.** 239, (1988) 321-331.

24. H. Angerstein-Koslowska, B. E. Conway, A. Hamelin, L. Stoicoviciu, **J. Electroanal. Chem.** 228, (1987) 429-453.

25. D. B. Parry, M. G. Samant, H. Seki, M. R. Philpott, and K. Ashley, manuscript in preparation.

26. V. D. Jovic, B. M. Jovic, R. Parsons, **J. Electroanal. Chem.** 290, (1990) 257-262.

27. A. A. Michri, A. G. Pshchenichnikov, and R. Kh. Burshtein, **Sov. Electrochem.** 8, (1972) 351.

28. M. Shay and S. Bruckenstein, **J. Electroanal. Chem.** 188, (1985) 131-136.

29. M. R. Philpott, **Journal de Physique Colloque** 44, No. C-10 (1983) 295-304.

30. G. Xiaoping, A. Hamelin, M. J. Weaver, **J. Chem. Phys.** 95, No. 9 (1991) 6993-6996.